Mem. Natl Inst. Polar Res., Spec. Issue, **55**, 1–39, 2001

Geochemical characteristics and tectonic setting of metamorphosed rocks in the Tugela terrane, Natal belt, South Africa

Makoto Arima[1], Keiji Tani[1], Shinichi Kawate[2] and Stephen T. Johnston[3]

[1]*Geological Institute, Yokohama National University, Yokohama 240-8501 (arima@ed.ynu.ac.jp)*
[2]*Musashi High School, Tokyo (kawate@fb3.so-net.ne.jp)*
[3]*School of Earth and Ocean Sciences, University of Victoria, Victoria, B.C., Canada (stj@uvic.ca)*

Abstract: The isotopically juvenile Tugela terrane, part of the Grenvillian Natal belt, southeastern Africa consists of a heterogeneous assemblage of regionally metamorphosed (upper amphibolite facies) mafic and felsic rocks. The Tugela terrane is divisible on the basis of lithology and structural style, from east to west, into four major thrust sheets referred to as the Nkomo, Madidima, Mandleni and Tugela sheets, respectively. The Tugela sheet includes the Kotongweni tonalite, a 15 km long body of coarsely crystalline garnetiferous hornblende meta-tonalite. Although strongly lineated and foliated, the intrusive contact of the tonalite with its amphibolite wall rocks remains recognizable, as are wallrock xenoliths within the intrusion. Geochemically, the tonalite is extremely depleted with very low abundance of Ta, Nb, rare earth elements (REE) and LIL elements, features considered diagnostic of arc-related igneous rocks. The lithological and geochemical characteristics of the tonalite and its amphibolite wallrocks suggest their formation in an intra-oceanic arc setting comparable to the present day Izu-Bonin arc. In contrast, amphibolites of the underlying Mandleni sheet are characterized by relatively high abundance of Nb, Ti, LIL and HFS elements more similar to the present day oceanic island basalt. The lithologically and geochemically distinct thrust sheets that comprise the oceanic Tugela terrane were each derived from distinct tectonic settings. The Kotongweni tonalite and its wall rocks, preserved in the Tugela sheet, provide a record of middle Proterozoic magmatic arc development prior to the obduction of the Natal belt onto the Kaapvaal craton at about 1.1 Ga.

key words: Natal, Tugela, Grenvillian, intra-oceanic arc, South Africa

1. Introduction

The Grenvillian-age Natal belt is located in the eastern part of South Africa. It is a part of the Proterozoic Namaqua-Natal mobile belt surrounding the southern margin of the Kaapvaal craton. The Natal belt has been thought as one of the juvenile continental fragments of the first super continent "Rodinia". The belt is divided into three terranes, each of them having distinct structural, lithologic, and tectonic characteristics (Thomas, 1989). They are from north to south, the Tugela, Mzumbe, and Margate terranes. The

Tugela terrane has long been interpreted as an ophiolite complex (accreted oceanic crust: Matthews, 1972; Matthew and Charlesworth, 1981) obducted onto the Kaapvaal craton, while the Mzumbe and Margate terranes have been thought of as deeply eroded magmatic arcs (Thomas, 1989; Thomas *et al.*, 1999).

During March 1998 and March and August 1999, field surveys were conducted in the Tugela terrane as parts of the Japan-South Africa Joint Research Program. The aims of this joint study were to map various lithologic units, to collect representative rock samples for geochemical and petrographic analyses, and finally to make protolith interpretation of the metamorphic rocks based on the integration of these field, geochemical and petrographic data. Detailed description of the modes of field occurrence and petrographic characteristics of various lithologic units in the Tugela terrane are to be published elsewhere. This paper reports geochemical data of various lithologic units that provide valuable constraints for estimation of their protoliths.

2. Geological setting

The Tugela terrane is composed of four separated tectonostratigraphic packages from east to west respectively referred to as the Nkomo, Madidima, Mandleni, and Tugela sheets (Matthews, 1972; Matthew and Charlesworth, 1981) (Fig. 1). In the Nkomo and Madidima sheets, thick successions of quartzo-feldspathic gneiss is the predominant lithologic units with subordinate amounts of metamorphosed sedimentary rocks and amphibolite, while the Mandleni and Tugela sheets consist of bimodal meta-igneous rocks (mafic-ultramafic meta-volcanic rock and felsic gneiss). Numbers of small bodies of ultramafic schists (serpentine- and talc-chlorite schist) are recognized in the Tugela terrane, thought to define imbricate thrust faults (Matthews, 1959; Harmer, 1979). The Madidima sheet consists of leucocratic biotite feldspathic gneiss with lesser amounts of amphibolite and metasedimentary gneiss. Details of lithology, structure and metamorphism of the Madidima and Mandleni sheets are given by Johnston *et al.* (2001b). New U-Pb geochronological data (SHRIMP and TIMS) along with details of stratigraphy and structural geology of the Tugela terrane are presented in this volume by Johnston *et al.* (2001a).

The Tugela sheet the highest tectonostratigraphic package within the Tugela terrane consists of two structurally distinct tectonic slices, the Manyane and Tuma slices (Matthew and Charlesworth, 1981). The Tuma slice is separated from the former by thrust faults. The Tuma slice is composed of metasedimentary rocks with subordinate amounts of metamorphosed basaltic pillow lavas and volcaniclastic rocks. The Manyane slice consists predominantly of amphibolite referred to as the Manyane amphibolite and subordinate amounts of metamorphosed gabbroic rocks.

The Kotongweni tonalite complex (Harmer, 1979; Johnston *et al.*, 1998), a 15 km long intrusive body of coarsely crystalline garnetiferous hornblende tonalitic gneiss, is exposed along the Tugela River (Fig. 1). Although strongly deformed, the intrusive contact of the tonalite with the Manyane amphibolites remains recognizable. The complex consists mainly of tonalitic rocks with subordinate amounts of gabbroic rock. Hornblende (Mg/(Mg+Fe)=0.40–0.50), plagioclase (An_{37-58}), quartz and garnet

($Alm_{65}Gro_{13}Pyr_{16}Spe_6$) are essential mineral constituents of both tonalite and gabbro. The deformation features of the tonalite complex suggest that it was intruded prior to the obduction of the Tugela sheet onto the Kaapvaal craton (Johnston *et al.*, 2001a). Several additional plutonic bodies are exposed in the Tugela sheet, including the mafic-ultramafic Tugela Rand and Macala complexes, the Ntabasongoma gabbroic intrusion, the Mkondene diorite, and the Dimane granite (Fig. 1) (Matthew and Charlesworth, 1981). They are thought to be younger intrusions on the basis of their structural features (Johnston *et al.*, 2001a).

The Mandleni sheet consists predominantly of felsic gneisses with lesser amounts of amphibolite (the Mandleni amphibolite). The Evuleka layered ultramafic intrusion (Wuth and Archer, 1986) and the Mambulu "massif" type anorthosite complex (Reynolds, 1986) intruded into the Mandleni felsic gneiss and amphibolite. Within the Madidima, Mandleni and Tugela sheets, large numbers of granitic sheets and dykes, referred to as the Wosi granitoid suite (Johnston *et al.*, 2001a) are recognized. They are weakly deformed (up to 30 m thick) intrusions consisting of trondhjemite, granite, quartz monzonite or two-mica granite.

3. Geochemistry

Two hundred and forty-seven samples were collected from the Madidima, Mandleni, and Tugela sheets (Appendix 1). Sample localities are given in Fig. 1. We paid special attention to collect rock samples representative of protolith composition. Central portions of thick homogeneous layer were taken for geochemical samples to avoid chemical modification during metamorphism and alteration. Amphibolites with thin felsic veins and heterogeneous migmatitic gneisses were excluded from geochemical analyses. We carried out XRF whole rock analyses for 141 metamorphosed igneous rocks, and made ICP-MS analyses for 43 rock samples. Major and trace element (Ba, Co, Cr, Cu, Nb, Ni, Rb, Sr, V, Y, Zn, Zr) abundance were determined with X-ray fluorescence (XRF)(RIGAKU RIX-3000) at the National Institute of Polar Research, Japan. The glass beads for major and trace element analyses were prepared from powdered samples that were diluted with five times by Lithium Borate ($Li_2B_4O_7$). The analytical procedure followed the methods by Motoyoshi and Shiraishi (1995) and Motoyoshi *et al.* (1996). Detection limits of major and trace elements are 0.01 wt% and 0.1 ppm, respectively. Trace elements (rare earth elements (REE), Li, Be, Rb, Y, Zr, Nb, Mo, Sn, Sb, Cs, Hf, Ta, Tl, Pb, Th, U) were analyzed by the ICP-MS (Inductivity-coupled plasma mass spectrometry) at the Department of Geology, Shimane University. Kimura *et al.* (1995) and Roser *et al.* (2000) described the methods used and precision of the analysis. Mineral analyses were carried out with an automated energy-dispersive electron microprobe (LINK QX2000J system) at the Geological Institute, Yokohama National University. Operating conditions were 15-kV and 0.15×10^{-10} ampere on Cobalt; beam diameter 2 μm. Analyses were reduced using the LINK ZAF-4/FLS correction program.

In this paper we describe whole rock compositions of mainly gabbroic to tonalitic rocks of the Kotongweni tonalite complex and Manyane amphibolites in the Tugela sheet, and amphibolites and Wosi granitic gneisses in the Madidima and Mandleni sheets. The whole rock compositions of various lithologic units are given in Appendices 2–9.

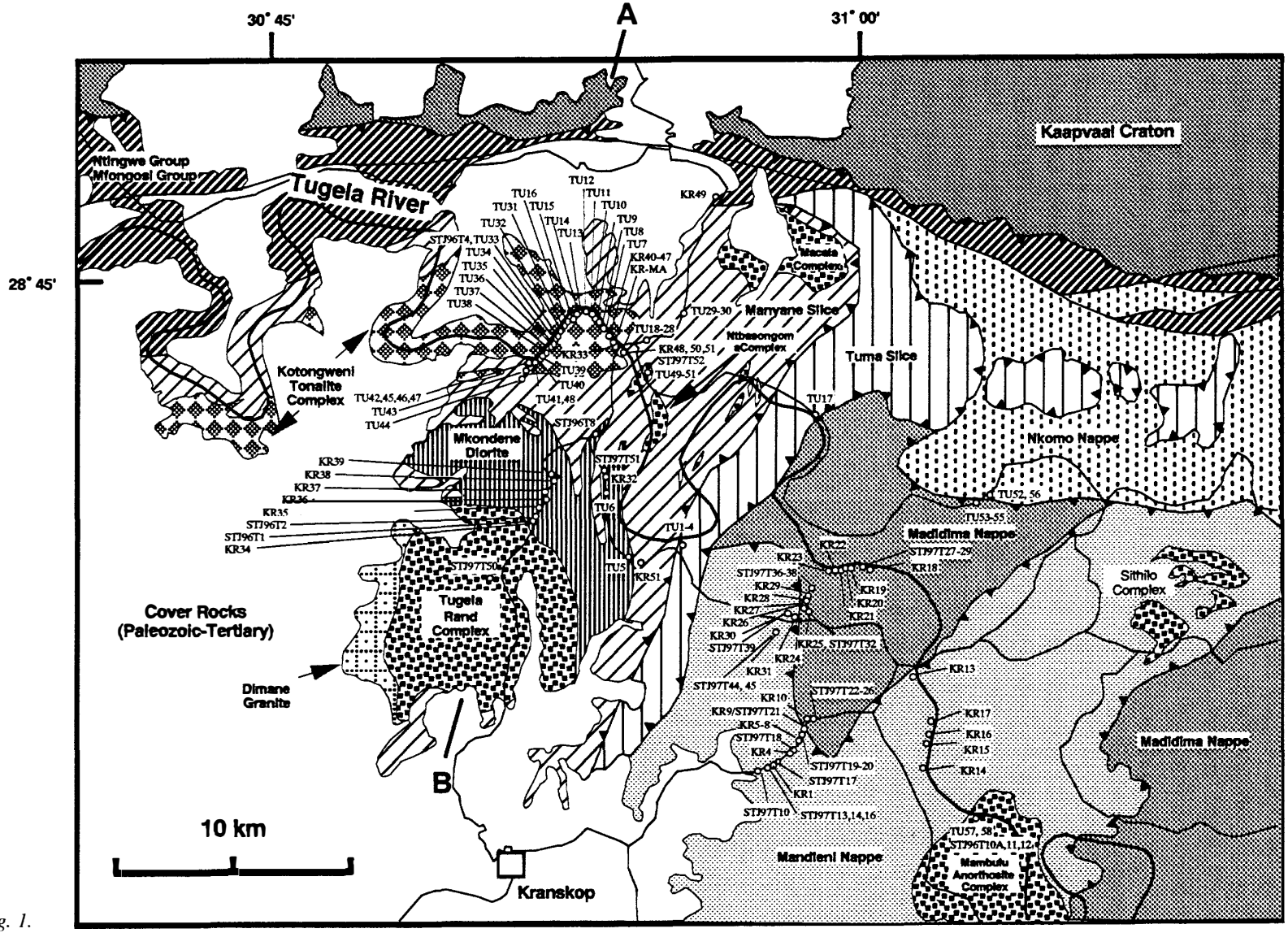
30° 45'
31° 00'
28° 45'
A
B
Kaapvaal Craton
Ntingwe Group
Mfongosi Group
Tugela River
Kotongweni Tonalite Complex
Mkondene Diorite
Cover Rocks (Paleozoic-Tertiary)
Dimane Granite
Tugela Rand Complex
Kranskop
10 km
Macala Complex
Manyane Slice
Ntbeongom aComplex
Tuma Slice
Nkomo Nappe
Madidima Nappe
Sithilo Complex
Madidima Nappe
Mandleni Nappe
Mambulu Anorthosite Complex
TU12
TU16
TU11
TU31
TU15
TU10
KR49
TU32
TU14
TU9
TU13
TU8
STJ96T4, TU33
TU7
TU34
KR40-47
KR-MA
TU35
TU36
TU37
TU38
TU29-30
TU18-28
KR48, 50,51
KR33
STJ97T52
TU39
TU49-51
TU40
TU42,45,46,47
TU41,48
TU17
TU43
TU44
STJ96T8
KR39
STJ97T51
KR38
KR32
KR37
KR36
TU6
KR35
TU1-4
STJ96T2
STJ96T1
KR34
TU5
KR51
KR22
KR23
KR18
KR19
KR29
KR28
KR20
KR27
KR21
KR26
KR30
KR25, STJ97T32
KR24
KR31
KR13
KR10
KR17
KR9/STJ97T21
KR16
KR5-8
KR15
KR4
KR14
KR1
TU57, 58
STJ96T10A,11,12,
TU52, 56
TU53-55
STJ97T27-29
STJ97T36-38
STJ97T39
STJ97T44, 45
STJ97T22-26
STJ97T18
STJ97T19-20
STJ97T17
STJ97T10
STJ97T13,14,16

Fig. 1.

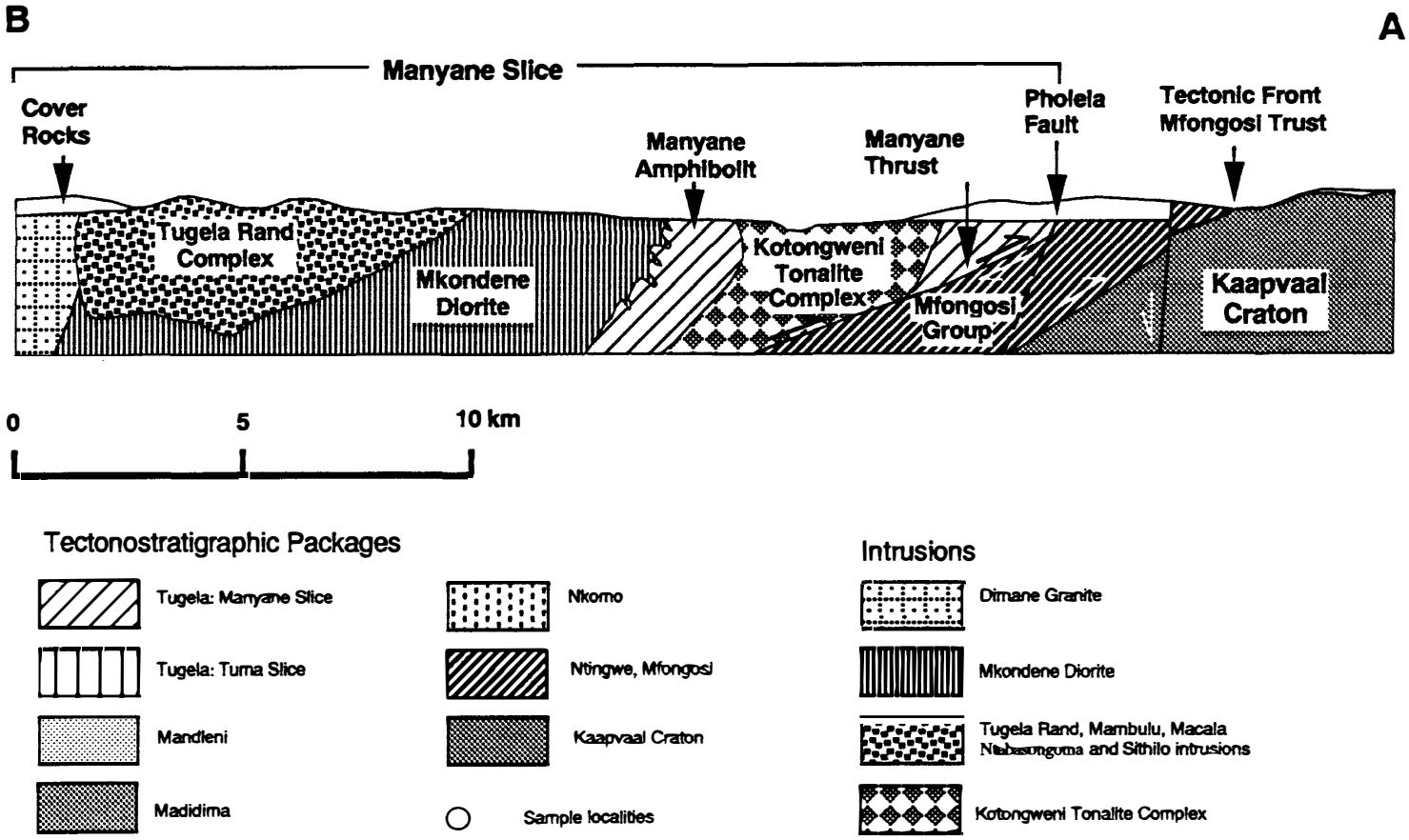

Fig. 1. Geological map of the Tugela terrane. Modified after Matthews and Charlesworth (1981).

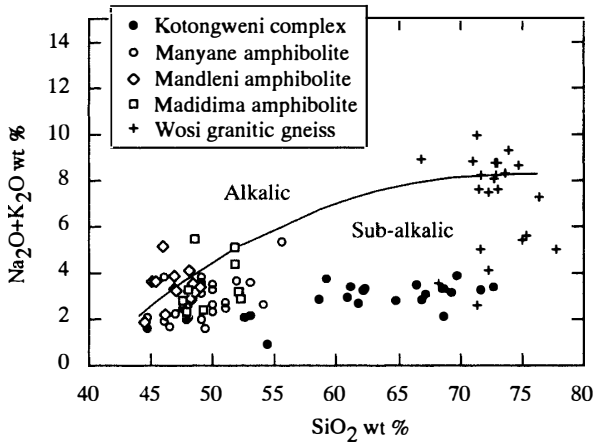

Fig. 2. Alkali-silica plots of amphibolites and granitic gneisses in the Tugela, Madidima and Mandleni sheets.

Amphibolites in the Tugela and Madidima sheets are within the sub-alkalic field while amphibolites in the Mandleni sheet occupy the alkalic field (Fig. 2). Bimodal distribution of metamorphosed igneous rocks in each sheet is well depicted in this figure. The Kotongweni tonalites plot in the sub-alkalic field in contrast to the majority of the Wosi granitic gneisses which have relatively high Na_2O and K_2O.

Changes in the abundance of major and trace elements in the Kotongweni tonalitic and gabbroic rocks are shown on the Harker variation diagrams of Figs. 3 and 4, respectively. The rocks belong to the calc-alkaline series and exhibit smooth and monotonous major element variations from 44 to 73 wt% SiO_2. Relatively low K_2O (<0.35 wt%) and K_2O/Na_2O (<0.23) are characteristic of all of the rocks analyzed (Appendix 2). These features are comparable to those reported from plutonic rocks in various oceanic island arcs such as the Izu arc (Kawate and Arima, 1998), Philippine (Wolfe *et al.*, 1978), New Britain (Whalen, 1985), Guadalcanal (Chivas *et al.*, 1982), Aleutian (Kay *et al.*, 1983), and Alaska (Barker, 1994). Most of the gabbroic rocks in the Kotongweni complex contain high MgO (up to 6.6 wt%), Al_2O_3 (up to 18.0 wt%) and CaO (up to 11.4 wt%) reflecting the high abundances of hornblende and plagioclase.

Trace element abundances in the rocks from the Kotongweni complex exhibit systematic trends with SiO_2 (Fig. 4). Nb shows constantly low abundance (<3 ppm). Compared with N-MORB (Pearce 1983), rocks of the Kotongweni complex are enriched in Sr, K, Rb, and Ba, and noticeably depleted in Nb, Zr, Ti and Y (Fig. 5), both of which are diagnostic features of rocks from subduction-related settings (Pearce, 1983). Relatively low REE abundances (1 to 10 times chondrite values), flat chondrite-normalized REE patterns are other characteristics of the Kotongweni rocks (Fig. 5). Relatively SiO_2-rich rocks in the Kotongweni complex exhibit a positive Eu anomaly suggesting plagioclase accumulation.

Three types of mafic enclaves are noted in the Kotongweni tonalite complex (Appendix 3). They are amphibolite-, gabbroic-, and hornblendite-enclave. Compositions of the amphibolite enclave are broadly comparable to those of the Manyane amphibolite (Figs. 3 and 4), implying the former is captured country rock of the Manyane amphibolite. The gabbroic- and hornblendite-enclave were probably derived from

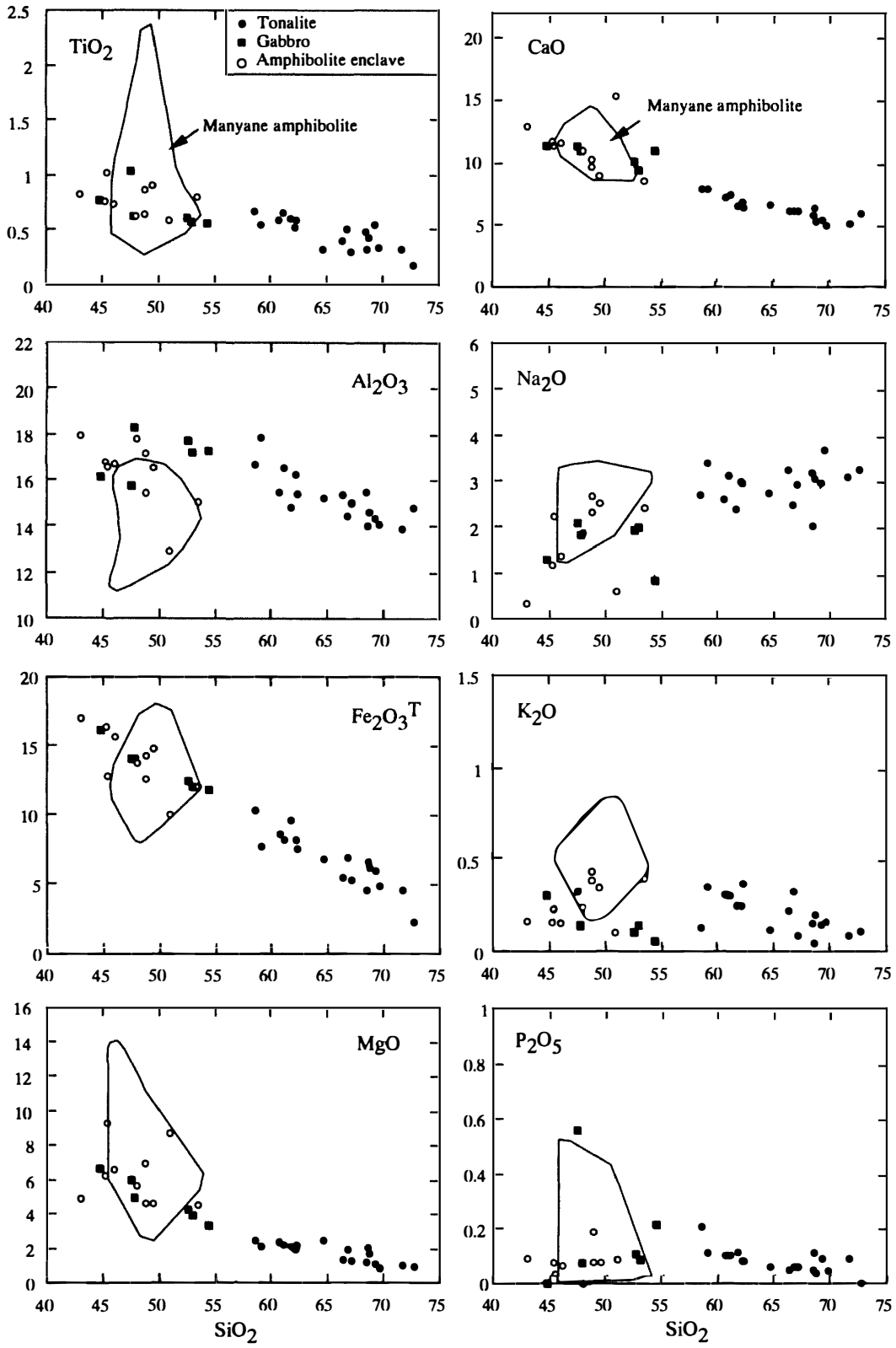

Fig. 3. Major element variations of tonalitic and gabbroic rocks of the Kotongweni tonalite complex. Amphibolite enclaves are comparable in chemistry to the Manyane amphibolite country rocks.

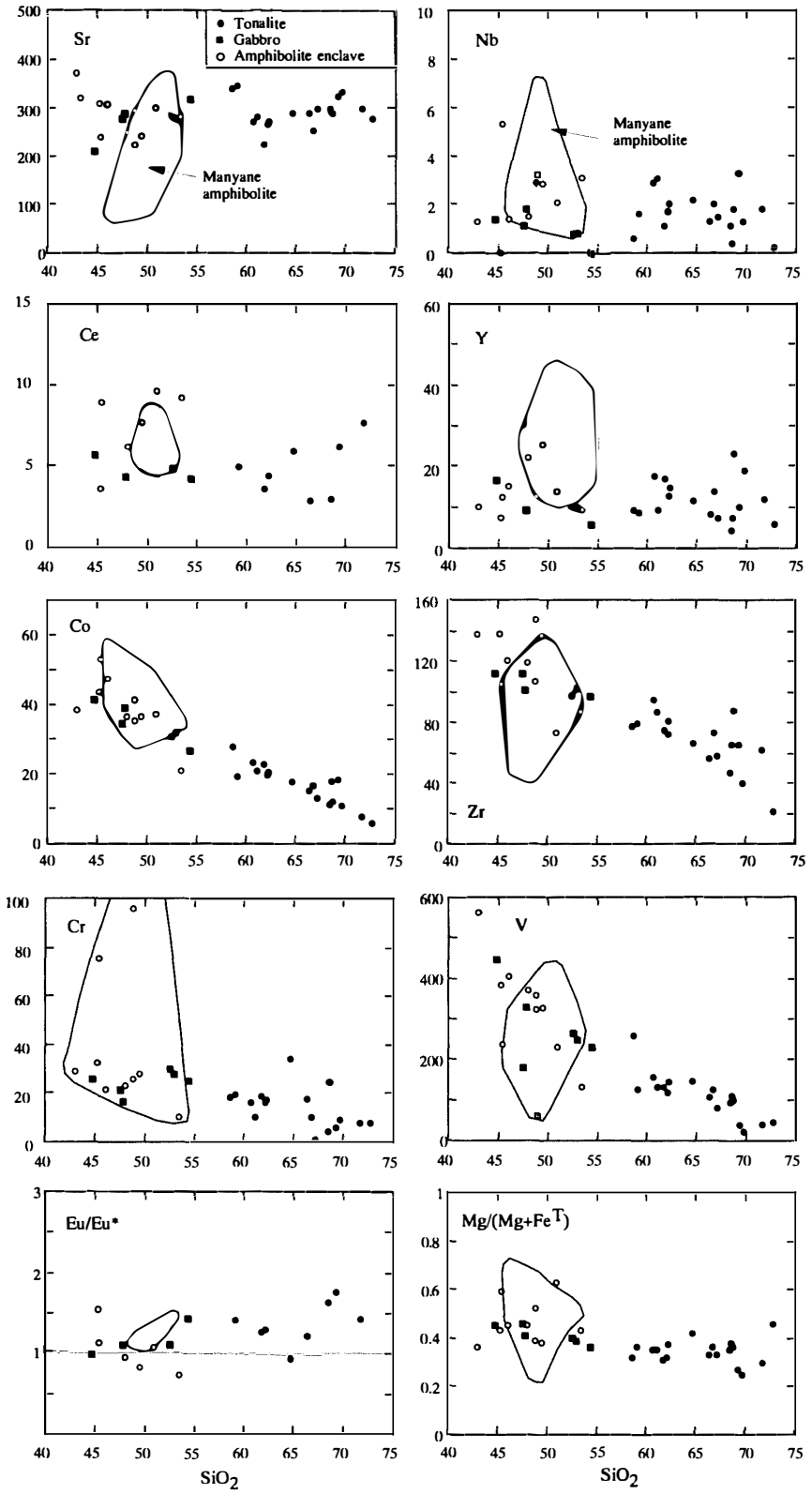

Fig. 4. Trace element variations of tonalitic and gabbroic rocks of the Kotongweni tonalite complex. Amphibolite enclaves are comparable in chemistry to the Manyane amphibolite country rocks.

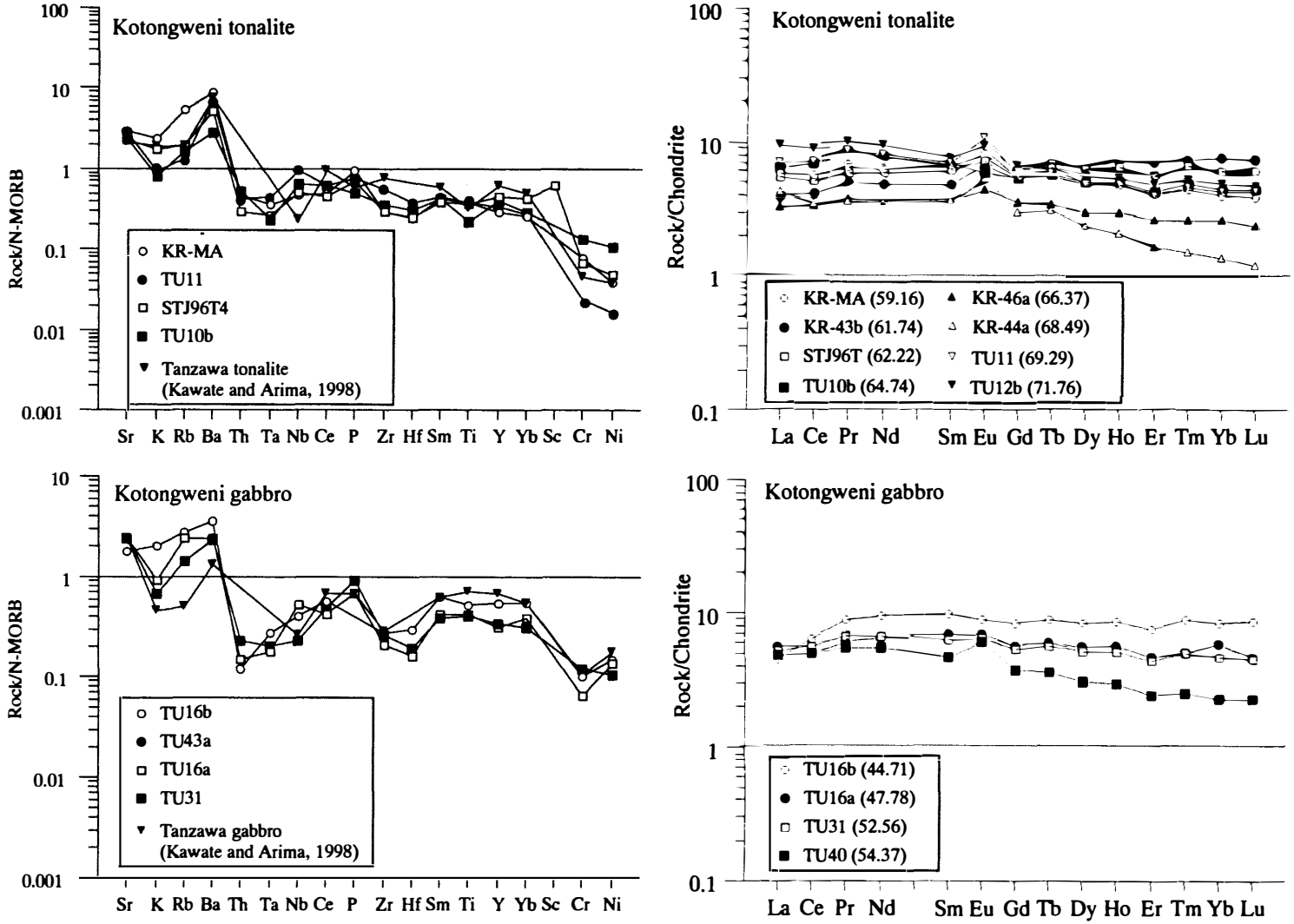

Fig. 5. MORB normalized Pearce plots and chondrite normalized REE plots of rocks of the Kotongweni complex. Tonalite and gabbro compositions of the Miocene Tanzawa complex, Izu arc are given for comparison. Values of the normalization constants are form Pearce (1983) for MORB and Nakamura (1974) for chondrite.

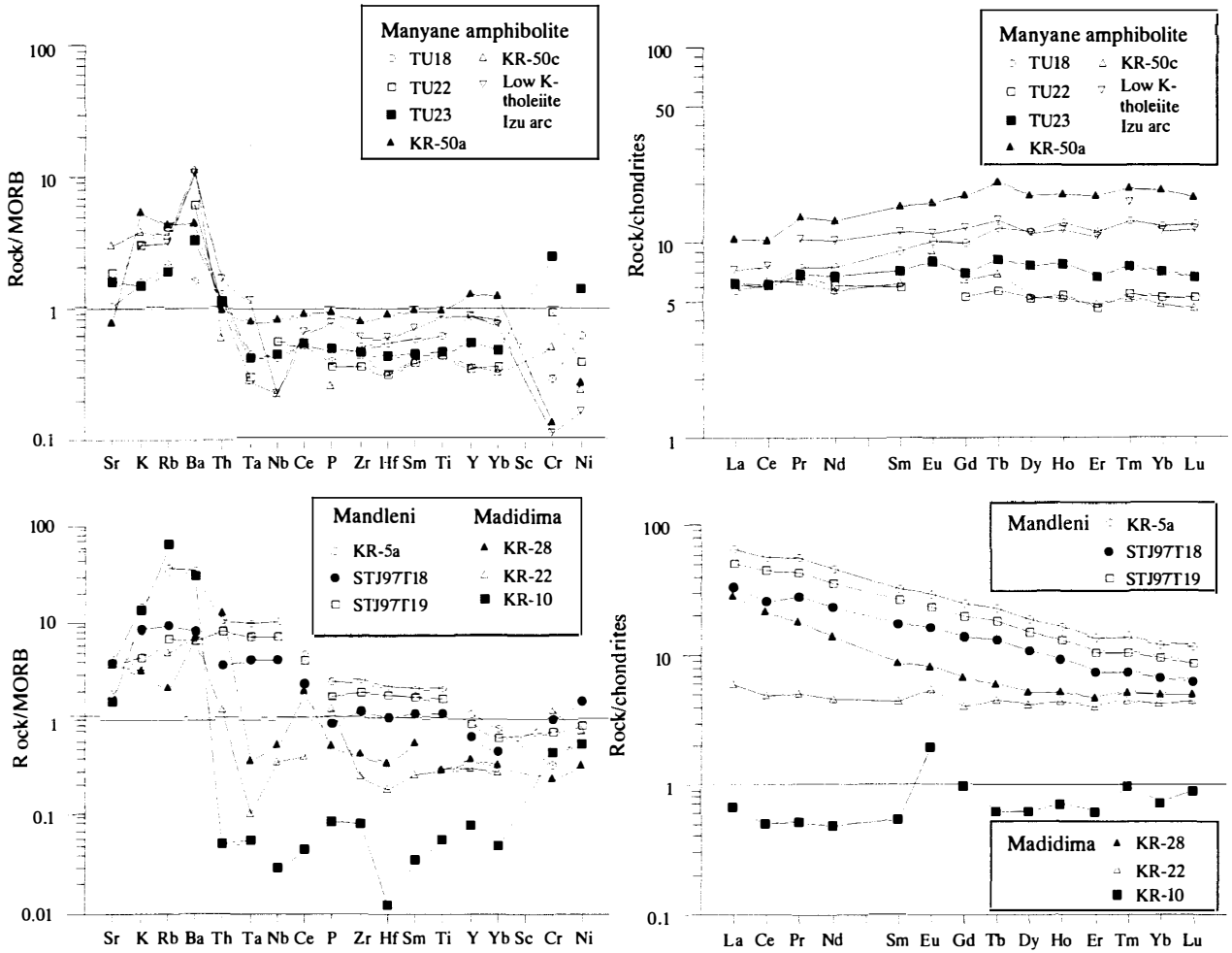

Fig. 6. MORB normalized Pearce plots and chondrite normalized REE plots of amphibolites in the Manyane slice of Tugela sheet together with amphibolites in the Mandleni and Madidima sheets. Low K-tholeiitic basalt composition of the Izu arc is given for comparison. Values of the normalization constants are form Pearce (1983) for MORB and Nakamura (1974) for chondrite.

Kotongweni tonalitic magma by crystal accumulation processes.

Whole rock compositions of the Manyane amphibolite (Appendix 4) are characterized by relatively high K, Ba, and Rb and low Ta, Nb, Zr and other HFS elements (Fig. 6). These features are comparable to those of the Kotongweni tonalite complex. These data suggest that the Manyane amphibolites were derived from low-K tholeiitic basaltic rocks that are chemically similar to those distributed in present day intra-oceanic arc systems (*cf.* Kawate and Arima, 1998). The Kotongweni tonalite and Manyane amphibolite wall rocks, preserved in the Tugela sheet, provide a record of middle Proterozoic intra-oceanic arc development prior to the obduction of the Natal belt onto the Kaapvaal Craton.

Distinct compositional difference exists between amphibolites in the Madidima sheet and those in the Mandleni sheet. Compared to MORB, the Madidima amphibolites are characterized by relatively low Ta, Nb, Ti and Zr and high K, Rb and Ba (Appendix 5), which are diagnostic features of rocks from subduction-related settings (Fig. 6)(Pearce, 1983). The Madidima amphibolite is interpreted as metamorphosed low-K arc tholeiitic basalts. In contrast, the Mandleni amphibolites exhibit relatively high abundance in both LIL and HSF elements (Fig. 6) and high Nb/Zr and Nb/Y ratios (Appendix 6, Fig. 7) that are indicative of their derivation from basaltic protoliths formed in a tectonic environment similar to present day oceanic islands (Pearce, 1983). Alternatively these "enriched" Mandleni amphibolites represent an anomalous magmatic event within the arc, possibly in response to the subduction of a spreading ridge and resulting development of a slab window. The chemistry of the Mandleni sheet is strikingly similar to the volcanics of southern Costa Rica and northern Panama which have been related to a slab window developed in response to the subduction of a portion of the Cocos-Nazca spreading ridge (see Johnston and Thorkelson, 1997).

The present data indicate that the lithologically and geochemically distinct thrust

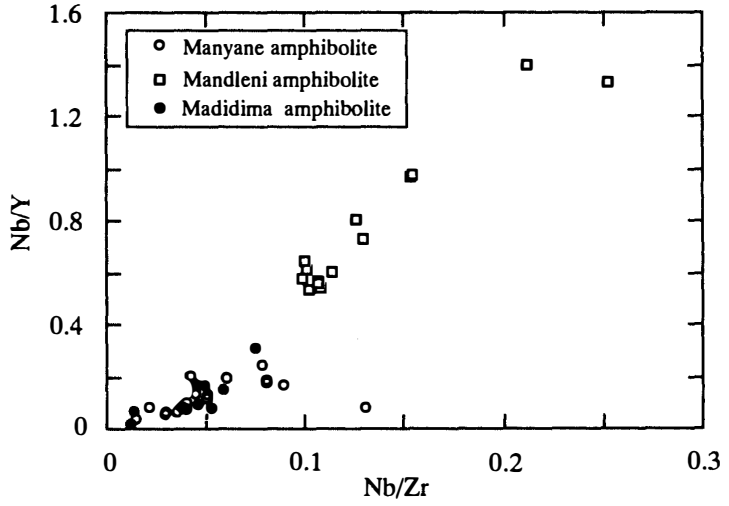

Fig. 7. Nb/Y vs. Nb/Zr plots of amphibolites of the Manyane, Mandleni, and Madidima sheets. The Mandleni amphibolites exhibit higher Nb/Y and Nb/Zr ratios and are comparable in composition to present day basaltic rocks occurring in the intra-oceanic plateau. The Manyane and Madidima amphibolites show relatively low Nb/Y and Nb/Zr ratios.

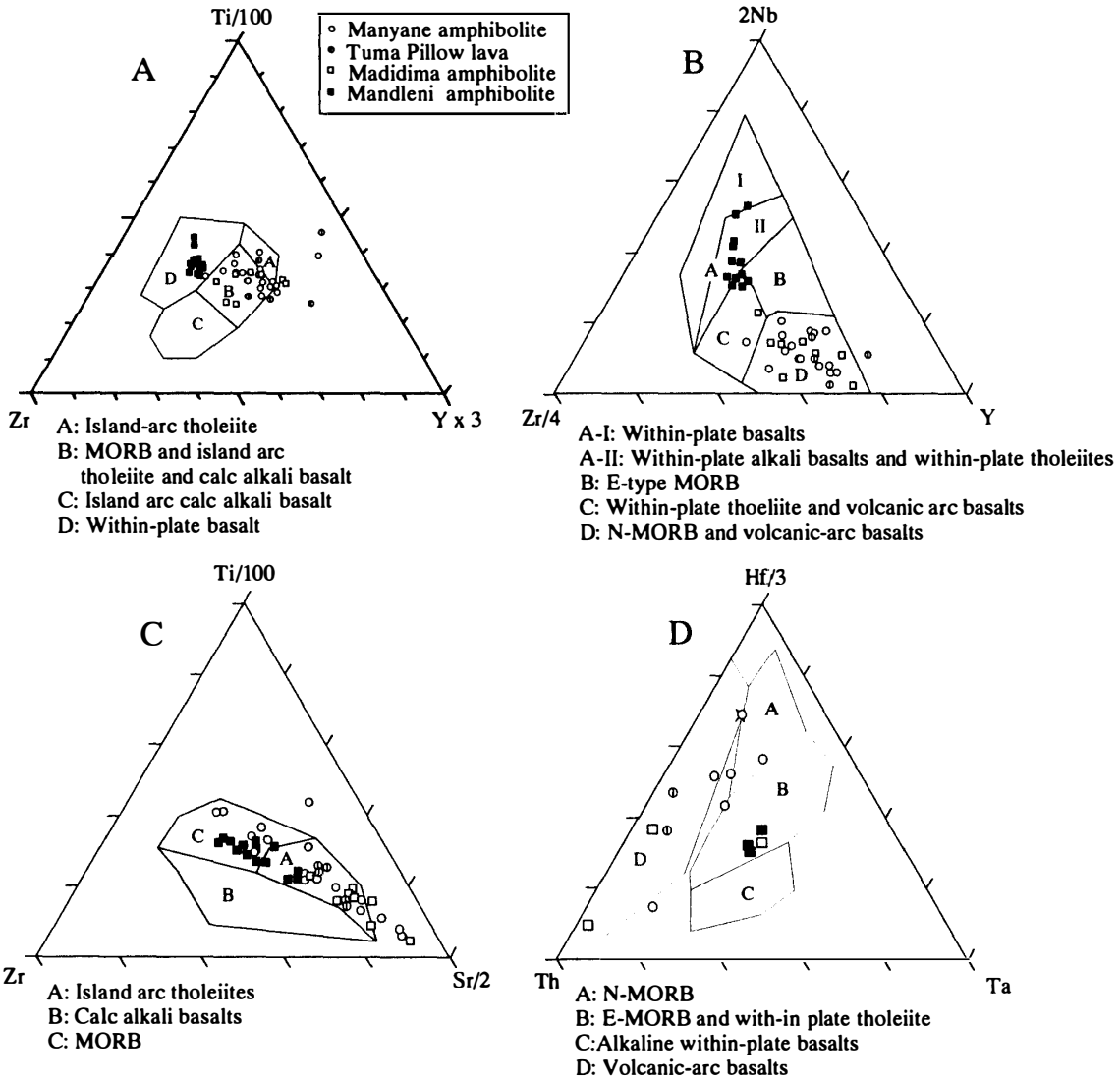

Fig. 8. Tectono-magmatism discrimination diagrams for the Manyane, Mandleni, and Madidima amphibolites. The data suggest "within-plate" tectono-magmatic signature for the Mandleni amphibolite. The Madidima and Manyane amphibolites are similar to arc-related basalts.

sheets that comprise the oceanic Tugela terrane were each derived from distinct tectonic settings. Plotting the present data in the various discrimination diagrams for basaltic composition (Fig. 8) supports this conclusion. In the Ti-Zr-Y (Pearce and Cann, 1973), Nb-Zr-Y (Meschede, 1986), Ti-Zr-Sr (Pearce and Cann, 1973) and Th-Hf-Ta (Wood, 1980) diagrams, the present data collectively suggest that the Mandleni amphibolite are metamorphosed basaltic rocks formed in an intra-plate setting (within-plate basalt) while the igneous protoliths of Manyane, Tuma and Madidima amphibolites were formed in a plate convergent environment.

The whole rock compositions of the Wosi granitic gneiss are given in Appendix 7. The Wosi granitic gneisses occupy the granite and trondhjemite fields and characterized by relatively high alumina saturation index (A.S.I.) (Fig. 9). Based on the SHRIMP U-Pb data (1155±1 Ma), the Wosi granite is interpreted as the syn-tectonic granite related to

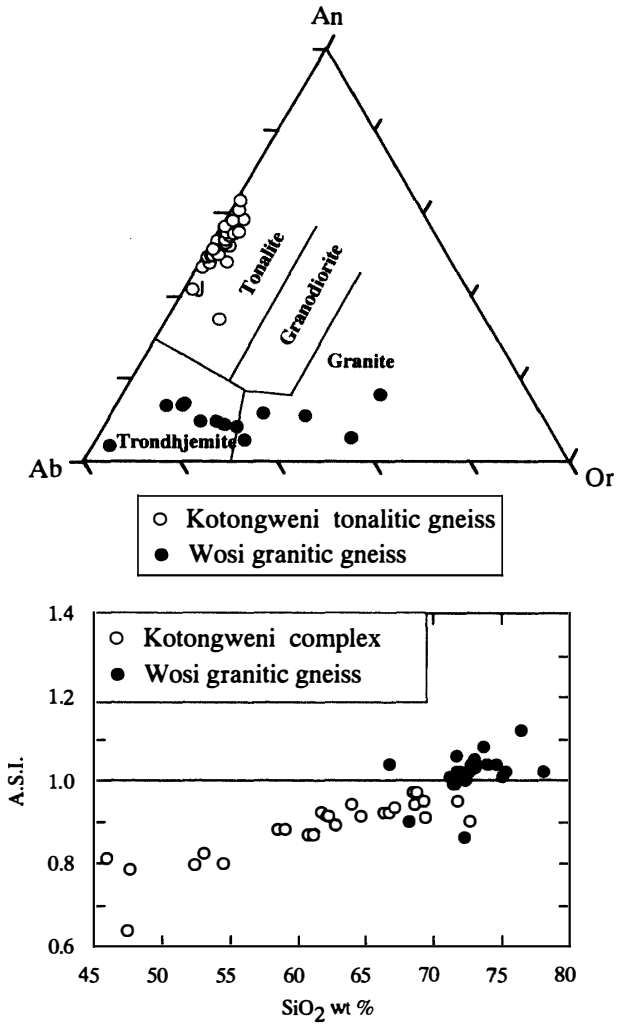

Fig. 9. Ternary An-Ab-Or plots and ASI vs. SiO_2 plots of the granitic rocks in the Tugela terrane. Marked difference exits between the Kotongweni tonalites in the Tugela sheet and Wosi granitic gneiss in the Madidima and Mandleni sheets.

the exhumation and obduction of the Natal belt onto the Kaapvaal craton (Johnston *et al.*, 2001a). Appendices 8 and 9 report whole rock compositions of the ultramafic schists in the Mandleni sheets and late stage mafic intrusions, respectively.

4. Discussion and conclusion

The data presented here clearly indicate that the Tugela terrane consists of thrust sheets, each of which has a distinct tectono-magmatic signature. The Tugela terrane is interpreted to be an accreted terrane consisting of rocks formed at intra-oceanic island arc and oceanic island (plateau) which are accreted to the continental margin of the Kaapvaal continent. It is likely that thrust faulting and metamorphism occurred during initial collision between the oceanic arc and ocean islands, and subsequently between the imbricated oceanic terranes and the continental margin of the Kaapvaal continent. In this

model, the ultramafic schists widely exposed along the thrust sheet boundaries are interpreted as supra-subduction zone ophiolites. The highly deformed Mfongosi and Ntingwe groups, distributed at the most northern margin of the Tugela terrane (Fig. 1), are interpreted as continental self deposits formed on the passive margin of the Kaapvaal craton. The Mfongosi and Ntingwe groups were probably incorporated within this accretionary complex during the Grenvillian continental-arc collision.

Combining the present data with data formerly reported, we speculate that the Natal belt, including the Mzumbe and Margate terranes, originated as a single intra-oceanic arc–the Natal arc. Arc magmatism is inferred to have developed in response to the subduction of oceanic crust of the Tugela ocean that separated the arc from the Kaapvaal craton. The polarity of subduction would be from the Kaapvaal craton toward the Natal arc (Jacobs and Thomas, 1994). The "Mandleni Oceanic Island or Plateau" once built on a foundation of oceanic crust of the Tugela ocean (Jacobs *et al.*, 1996) accreted to the Natal arc during closure of the Tugela (Fig. 10). The modern analogue to this Grenvillian continent-arc collision would be the Banda arc that is nearly colliding to the Australian continent at the Java trench (Hamilton, 1979).

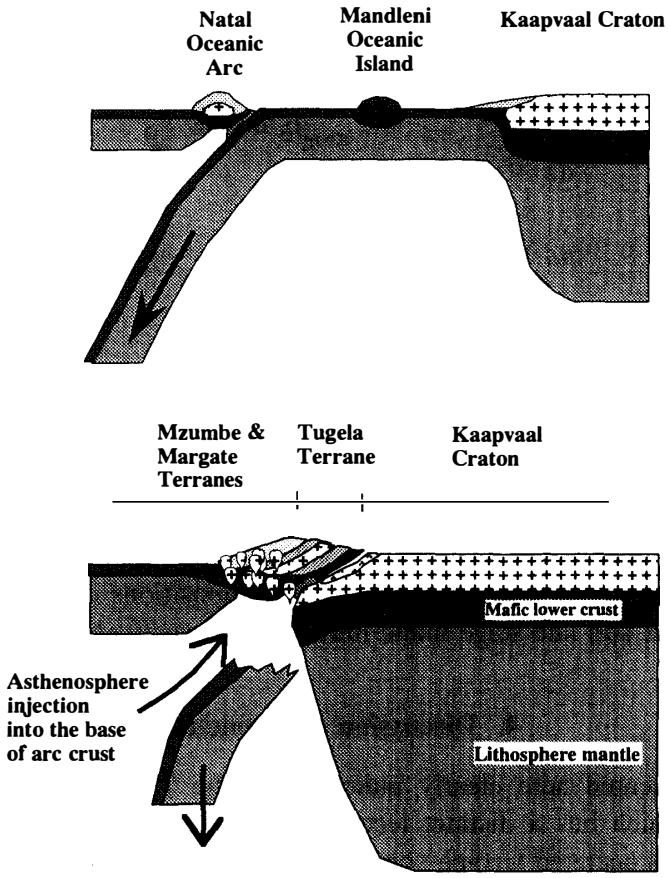

Fig. 10. Schematic sketch illustrating crust formation of the Tugela terrane during Grenvillian continent-arc collision. The Tugela terrane is interpreted as an accretionary complex composed of intra-oceanic "Natal Arc" and accreted "Mandleni Oceanic Island" during closure of the "Tugela Ocean" that once separated the Natal arc from the Kaapvaal continent.

Acknowledgments

We thank K. Shiraishi, Y. Motoyoshi, Y. Hiroi, N. Tsuchiya, and S. McCourt for insightful discussions. We wish to thank Geoff Grantham for his critical review and comments. We are greatly indebted to J. Kimura for providing ICP-MS analytical support. We also thank A. Bisnath for field assistance and K. Seno for XRF technical assistance. This study is a part of the Japan-South Africa Joint Research Program funded by Grant in Aid for General Scientific Research (GAGSR) from the Ministry of Education, Science and Culture to Professor K. Shiraishi, National Institution of Polar Research. The parts of this study are also funded by GAGSR (08454154 and 12440147) to M. Arima.

References

Barker, F. (1994): Some accreted volcanic rocks of Alaska and their elemental abundances. The Geology of North America, Vol. G-1, ed. by G. Plafker and H.C. Berg. Boulder, Geological Society of America, 555–587.

Chivas, A.R., Andrew, A.S., Sinha, A.K. and O'Niel, J.R. (1982): Geochemistry of a Pliocene-Pleistocene oceanic plutonic complex, Guadalcanal. Nature, **300**, 139–143.

Hamilton, W. (1979): Tectonics of the Indonesian Region. U.S. Geol Surv. Prof. Pap., 1078 p.

Harmer, R.E. (1979): Pre-cape Geology of the Tugela valley north of Kranskop, Natal. Unpubl. M.Sc. thesis, University of Natal, 234 p.

Jacobs, J. and Thomas, R.J. (1996): Pan-African rejuvenation of the *c.* 1.1 Ga Natal Metamorphic Province (South Africa): K-Ar muscovite and titanite fission track evidence. J. Geol. Soc. London, **153**, 971–978.

Jacobs, J. and Thomas, R.J. (1994): Oblique collision at about 1.1 Ga along the southern margin of the Kaapvaal continent, south-east Africa. Geol. Rundsch, **83**, 322–333.

Johnston, S.T. and Thorkelson, D.J. (1997): Cocos-Nazca slab window beneath Central America. Earth Planet. Sci., **146**, 465–474.

Johnston, S.T., Arima, M., Kawate, S., Shiraishi, K., Kimura, J. and McCourt, S. (1998): The Kotongweni tonalite, Tugela terrane, southeastern Africa: The plutonic root of a Grenvillian oceanic arc. GSA Ann. 1998 Meeting, Toronto, 259.

Johnston, S.T., Armstrong, R., Heaman, L., McCourt, S., Mitchell, A., Bisnath, A. and Arima, M. (2001a): Preliminary U-Pb geochronology of the Tugela terrane, Natal belt, eastern South Africa. Mem. Natl Inst. Polar Res., Spec. Issue, **55**, 40–58.

Johnston, S.T., McCourt, S., Bisnath, A. and Mitchell, A. (2001b): The Tugela terrane Natal tectonic belt: Kibaran magmatism and tectonism along the south-east margin of the Kaapvaal craton. submitted to S. Afr. J. Geol.

Kay, S.M., Kay, R.W., Brueckner, H.K. and Rubenstone, J. (1983): Tholeiitic Aleutian arc plutonism: The Finger Bay pluton, Adak Island, Alaska. Contrib. Mineral. Petrol., **82**, 99–116.

Kawate, S. and Arima, M. (1998): Petrogenesis of the Tanzawa plutonic complex, central Japan: Exposed felsic middle crust of the Izu-Bonin-Mariana arc. Island Arc, **7**, 342–358.

Kimura, J-I., Takaku, Y. and Yoshida, T. (1995): Igneous rock analysis using ICP-MS with internal standardization, isobaric ion overlap correction, and standard addition methods. Sci. Rep. Fukushima Univ., **56**, 1–12.

Matthews, P.E. (1959): The metamorphism and tectonics of the pre-cape formations in the post-ntingwe thrust-belt, S.W. Zululand, Natal. Trans. Geol. Soc. S. Afr., **62**, 257–322.

Matthews, P.E. (1972): Possible Precambrian obduction and plate tectonics in southeastern Africa. Nature, **240**, 37–39.

Matthews, P.E. and Charlesworth, E.G. (1981): Northern margin of the Namaqua–Natal mobile belt in

Natal. Durban, South Africa, University of Natal.
Meschede, M. (1986): A method of discriminating between different types of mid-ocean ridge basalts and continental tholeiites with the Nb-Zr-Y diagram. Chem. Geol., **56**, 207–218.
Motoyoshi, Y. and Shiraishi, K. (1995): Quantitative chemical analyses of rocks with X-ray fluorescence analyzer: (1) Major elements. Nankyoku Shiryô (Antarct. Rec.), **39**, 40–48 (in Japanese with English abstract).
Motoyoshi, Y., Ishizuka, H. and Shiraishi, K. (1996): Quantitative chemical analyses of rocks with X-ray fluorescence analyzer: (2) Trace elements. Nankyoku Shiryô (Antarct. Rec.), **40**, 53–63 (in Japanese with English abstract).
Nakamura, N. (1974): Determination of REE, Ba, Fe, Mg, Na and K in carbonaceous and ordinary chondrites. Geochim. Cosmochim. Acta, **38**, 757–773.
Pearce. J.A. (1983): Role of the sub-continental lithosphere in magma genesis at active continental margins. Continental Basalts and Mantle Xenoliths, ed. by C.J. Hawkesworth and M.J. Norry. Shiva, Nantwich, 230–249.
Pearce, J.A. and Cann, J.R. (1973): Tectonic setting of basaltic rocks determined using trace element analyses. Earth Planet. Sci. Lett., **19**, 290–300.
Reynolds, I.M. (1986): The mineralogy and petrography of some vanadium-bearing titaniferous iron ores of the Mambula complex, Zululand. Mineral Deposits of Southern Africa, Vol. 2, ed. by C.R. Anhaeusser and S. Maske. Johannesburg, Geological Society of South Africa, 1695–1708.
Roser B.P., Kimura, J.-I. and Hisatomi, K. (2000): Whole-rock elemental abundances in sandstones and mudrocks from the Tanabe Group, Kii Peninsula, Japan. Sci. Rep. Shimane Univ., **19**, 101–112.
Thomas, R.J. (1989): A tale of two tectonic terranes. S. Afr. J. Geol., **92**, 306–321.
Thomas, R.J., Cornell, D.H. and Armstrong, R.A. (1999): Provenance age and metamorphic history of the Quha Formation, Natal Metamorphic Province: a U-Th-Pb zircon SHRIMP study. S. Afr. J. Geol., **102**, 83–88.
Whalen, J.B. (1985): Geochemistry of an island-arc plutonic suite: the Uasilau-Yau Yau intrusive complex, New Britain, P. N. G. J. Petrol., **26**, 603–632.
Wolfe, J.A., Magnuson, M.S. and Divis, A.F. (1978): The Taysan porphyry copper deposit, southern Luzon island, Philippines. Econ. Geol., **73**, 605–617.
Wood, D.A. (1980): The application of a Th-Hf-Ta diagram to problems of tectonomagmatic classification and to establishing the nature of crustal contamination of basaltic lavas of the British Tertiary volcanic province. Earth Planet. Sci. Lett., **50**, 11–30.
Wuth, M.G. and Archer, P.D. (1986): Chromite mineralization at Sithilo, Northern Zululand. Mineral Deposits of Southern Africa, Vol. 2, ed. by C.R. Anhaeusser and S. Maske. Johannesburg, Geological Society of South Africa, 1689–1694.

(Received March 16, 2001; Revised manuscript accepted May 9, 2001)

Appendix 1. Sample list.

Sample No.	Rock Type	Thrust sheet and lithological units	Remarks
STJ96TT3	metabasite	Mapumulo	
STJ96TT8	hbl-pl gneiss	Matigulu	
STJ96TT12	granitic dyke	Matigulu	
STJ96TT13B	tonalitic gneiss	Matigulu	
STJ96T1	hyp bi diorite	Mkondene	
STJ96T2	bi qtz diorite	Mkondene	
STJ96T4	grt tonalitic gneiss	Kotongweni	
STJ96T8	hbl qtz diorite	Mkondene	
STJ96T10A	sheared anorthosite	Mambulu	
STJ97T10	pegmatitic granite	Mandleni	
STJ97T11	felsic gneiss	Mambulu	
STJ97T12	pyroxene gabbronorite	Mambulu	
STJ97T13	mica feldspathic gneiss	Mandleni	
STJ97T14	grey gneiss	Mandleni	intermidiate
STJ97T16	grey banded gneiss	Mandleni	
STJ97T17	mus granitic gneiss	Mandleni	
STJ97T18	ep amphibolite	Mandleni	High Ti-Nb amphibolite
STJ97T19	amphibolite	Mandleni	High Ti-Nb amphibolite
STJ97T20	mus feldspathic gneiss	Mandleni	
STJ97T21	talc schist	Mandleni	
STJ97T22	hbl schist	Madidima	ultlamafic schist
STJ97T23	talc schist	Madidima	
STJ97T24	amphibolite	Madidima	Low Ti-Nb amphibolite
STJ97T25	amphibolite	Madidima	Low Ti-Nb amphibolite
STJ97T26	grey gneiss	Madidima	intermidiate
STJ97T27	bi m grey gneiss	Madidima	
STJ97T28	granitic gneiss	Madidima	
STJ97T29	amphibolite	Madidima	Low Ti-Nb amphibolite
STJ97T30	mu bi feldspathic gneiss	Madidima	
STJ97T31	mica ceous granite	Madidima	
STJ97T32	bi feldspathic gneiss	Madidima	
STJ97T33	bi qtz diorite	Madidima	
STJ97T34	ultlamafic schist	Madidima	
STJ97T35	ultramafic schist	Madidima	
STJ97T36	calc-silicate gneiss	Madidima	
STJ97T37	felsic dyke	Madidima	
STJ97T38	grey bi gneiss	Madidima	
STJ97T39	banded amphibolite	Madidima	Low Ti-Nb amphibolite
STJ97T40	hornblendite	Madidima	
STJ97T41	bi leucogneiss	Madidima	
STJ97T42	amphibolite	Madidima	Low Ti-Nb amphibolite
STJ97T43	bi leucogneiss	Mandleni	
STJ97T44	bi leucogneiss	Mandleni	
STJ97T45	metabasite gneiss	Mandleni	intermidiate
STJ97T46	talc schist	Mandleni	
STJ97T50	pegmatitic pyroxenite	Tugela Rand	
STJ97T51	bi opx diorite	Mkondene	
STJ97T52	amphibolite	Manyane	country rock
STJ97T10-KR	pegmatitic granite	Mandleni	

Appendix 1. Sample list (continued).

sample No.	Rock Type	Thrust sheet and lithological units	Remarks
KR-1a	amphibolite	Mandleni	High Ti-Nb amphibolite
KR-1b	amphibolite	Mandleni	High Ti-Nb amphibolite
KR-1c	felsic gneiss	Mandleni	
STJ97T18-KR	amphibolite	Mandleni	High Ti-Nb amphibolite
KR-4a	amphibolite	Mandleni	
KR-4b	felsic gneiss	Mandleni	
KR-5a	amphibolite	Mandleni	High Ti-Nb amphibolite
KR-5b	granitic gneiss	Mandleni	
KR-6	amphibolite	Mandleni	
STJ97T19-KR	amphibolite	Mandleni	High Ti-Nb amphibolite
KR-7	amphibolite	Mandleni	High Ti-Nb amphibolite
STJ97T20-KR	mu feldspathic gneiss	Mandleni	
KR-8a	felsic gneiss (host)	Mandleni	
KR-8b	felsic gneiss (enclave)	Mandleni	
KR-8c	granitic gneiss	Mandleni	
KR-9a	serpentinite (dark green)	Mandleni	ultlamafic schist
KR-9b	serpentinite (light green)	Mandleni	ultlamafic schist
KR-9c	talc schist	Mandleni	
KR-9d	serpentinite (fine grained)	Mandleni	ultlamafic schist
KR-9e	talc schist	Mandleni	
STJ97T24-KR	amphibolite	Madidima	Low Ti-Nb amphibolite
STJ97T23-KR	talc schist	Madidima	
STJ97T22-KR	hornblende schist	Madidima	
KR-10	amphibolite	Madidima	Low Ti-Nb amphibolite
KR-11	ultlamafic schist	Madidima	
KR-12a	gray gneiss	Madidima	intermidiate
KR-12b	granitic gneiss	Madidima	
KR-13a	granitic gneiss	Mandleni	
KR-13b	amphibolite	Mandleni	High Ti-Nb amphibolite
KR-13c	amphibolite	Mandleni	High Ti-Nb amphibolite
KR-13d	amphibolite	Mandleni	High Ti-Nb amphibolite
KR-13e	granitic gneiss	Mandleni	
KR-14a	felsic gneiss	Mandleni	
KR-14b	amphibolite	Mandleni	High Ti-Nb amphibolite
KR-14c	felsic gneiss	Mandleni	
KR-15	amphibolite	Mandleni	High Ti-Nb amphibolite
KR-16	felsic gneiss	Mandleni	
KR-17	amphibolite	Mandleni	High Ti-Nb amphibolite
KR-18a	calk-silicate gneiss	Madidima	
KR-18b	muscovite rich gneiss	Madidima	felsic gneiss
KR-18c	amphibolite	Madidima	
KR-18d	felsic gneiss	Madidima	
KR-18e	grt bearing granitic gneiss	Madidima	
STJ97T27-KR	intermidiate gneiss	Madidima	
KR-19	pegmatite (grt-rich)	Madidima	
KR-20	garnet rich metasedimant	Madidima	
KR-21	amphibolite	Madidima	Low Ti-Nb amphibolite
KR-22	amphibolite	Madidima	Low Ti-Nb amphibolite
KR-23	intermidiate gneiss	Madidima	
KR-24	amphibolite	Mandleni	High Ti-Nb amphibolite

Appendix 1. Sample list (continued).

sample No.	Rock Type	Thrust sheet and lithological units	Remarks
STJ97T32-KR	intermidiate gneiss	Madidima	
KR-25	bio pl gneiss	Madidima	
KR-26	bio grt gneiss	Madidima	
KR-27	granulite banded gneiss	Madidima	
KR-28	amphibolite	Madidima	Low Ti-Nb amphibolite
KR-29	dolerite dike	Karoo	
KR-30a	amphibolite	Mandleni	High Ti-Nb amphibolite
KR-30b	intermidiate gneiss	Mandleni	
KR-30c	greenish layer	Mandleni	
KR-31a	felsic gneiss	Mandleni	
KR-31b	amphibolite	Mandleni	
KR-31c	felsic gneiss	Mandleni	
KR-32	amphibolite	Manyane	wall rock
KR-33a	grt tonalitic gneiss	Kotongweni	
KR-33b	amphibolite	Kotongweni	wall rock
KR-34	hyp hbd qtz diorite	Mkondene	
KR-35	diorite	Mkondene	
KR-36	diorite	Mkondene	
KR-37a	enclave	Mkondene	
KR-37b	enclave	Mkondene	
KR-38	diorite	Mkondene	
KR-39a	enclave	Mkondene	
KR-39b	diorite	Mkondene	
KR-40a	amphibolite (coarse)	Kotongweni	enclave
KR-40b	amphibolite (fine)	Kotongweni	enclave
KR-40c	amphibolite (coarse)	Kotongweni	enclave
KR-40d	amphibolite (fine)	Kotongweni	enclave
KR-40e	amphibolite (fine)	Kotongweni	enclave
KR-41	hornblendite	Kotongweni	enclave
KR-42a	meta-sediment	Kotongweni	enclave
KR-42b	grt tonalitic gneiss	Kotongweni	
KR-43a	amphibolite	Kotongweni	enclave
KR-43b	grt tonalitic gneiss	Kotongweni	
KR-MA	grt tonalitic gneiss	Kotongweni	
KR-44a	grt tonalitic gneiss	Kotongweni	
KR-44b	amphibolite	Kotongweni	enclave
KR-45a	grt tonalitic gneiss	Kotongweni	
KR-45b	amphibolite	Kotongweni	enclave
KR-46a	tonalitic gneiss	Kotongweni	
KR-46b	amphibolite	Kotongweni	enclave
KR-47	gabbroic gneiss	Kotongweni	enclave
KR-48a	amphibolite	Manyane	
KR-48b	amphibolite	Manyane	
KR-49	basalt	Mfongosi	lava
KR-50a	amphibolite	Manyane	
KR-50b	amphibolite	Manyane	
KR-50c	amphibolite	Manyane	
KR-51a	amphibolite	Manyane	
KR-51b	amphibolite	Manyane	

Appendix 1. Sample list (continued).

sample No.	Rock Type	Thrust sheet and lithological units	Remarks
KR-51c	amphibolite (with vein)	Manyane	
KR-51d	amphibolite	Manyane	
TU-1a	felsic schist (mica rich)	Tuma	
TU-1b	mafic schist	Tuma	
TU-1c	felsic schist	Tuma	
TU-1d	grt-metasediment	Tuma	
TU-2	biotite gneiss	Tuma	
TU-3	metasediment	Tuma	
TU-4	mafic gneiss	Tuma	
TU-5	intermidiate gneiss	Manyane	
TU-6	diorite	Mkondene	
TU-7a	grt tonalitic gneiss	Kotongweni	
TU-7b	amphibolite	Kotongweni	enclave
TU-7c	gabbro	Kotongweni	enclave
TU-8a	amphibolite	Kotongweni	enclave
TU-8b	grt tonalitic gneiss	Kotongweni	
TU-9	grt tonalitic gneiss	Kotongweni	
TU-10a	grt tonalitic gneiss	Kotongweni	
TU-10b	grt tonalitic gneiss	Kotongweni	
TU-10c	amphibolite	Kotongweni	enclave
TU-11	grt tonalitic gneiss	Kotongweni	
TU-12a	grt tonalitic gneiss	Kotongweni	
TU-12b	grt tonalitic gneiss	Kotongweni	
TU-13	grt tonalitic gneiss	Kotongweni	
TU-14a	gabbro	Kotongweni	enclave
TU-14b	grt tonalitic gneiss	Kotongweni	
TU-15	grt tonalitic gneiss	Kotongweni	
TU-16a	gabbroic gneiss	Kotongweni	
TU-16b	gabbroic gneiss	Kotongweni	
TU-17a	mafic schist	Tuma	pillow lava
TU-17b	metapelite (bi-gar)	Tuma	garnet-bearing
TU-17c1	metapelite	Tuma	
TU-17c2	amphibolite	Tuma	
TU-17d	metapelite (gar)	Tuma	garnet-bearing
TU-17e	metapelite (felsic part)	Tuma	felsic
TU-17f	metapelite (gar)	Tuma	garnet-bearing
TU-17g	metapelite (bio-rich)	Tuma	biotite rich
TU-17h	metapelite	Tuma	
TU-17i	metapelite	Tuma	biotite rich
TU-17j	metapelite	Tuma	mafic
TU-17k	metapelite (mafic part)	Tuma	mafic
TU-17l	amphibolite	Tuma	
TU-17m	feldspasic gneiss	Tuma	metasediment
TU-17n	pegmatite	Tuma	
TU-17o	mafic schist	Tuma	pillow lava
TU-17p	mafic schist	Tuma	pillow lava
TU-17q	amphibolite	Tuma	
TU-17r	amphibolite	Tuma	
TU-17s	meta-sandstone	Tuma	

Appendix 1. Sample list (continued).

sample No.	Rock Type	Thrust sheet and lithological units	Remarks
TU-17t	meta-sandstone	Tuma	arenite like
TU-17u1	mafic schist	Tuma	pillow lava
TU-17u2	mafic schist	Tuma	pillow lava
TU-18	amphibolite	Manyane	
TU-19	metagabbro (coarse)	Manyane	
TU-20	gabbroic dyke	Manyane	
TU-21	tonalitic intrusion	Manyane	
TU-22	amphibolite	Manyane	
TU-23	metagabbro	Manyane	
TU-24	metagabbro	Manyane	
TU-25	mafic dyke	Manyane	
TU-26	amphibolite	Manyane	
TU-27	gabbroic dyke	Manyane	
TU-28	amphibolite	Manyane	
TU-29	amphibolite	Manyane	
TU-30	amphibolite	Manyane	
TU-31	gabbroic gneiss	Kotongweni	
TU-32	gabbroic gneiss	Kotongweni	
TU-33	hornblendite	Kotongweni	enclave
TU-34a	hornblendite	Kotongweni	enclave
TU-34b	tonalitic gneiss	Kotongweni	
TU-35	amphibolite	Kotongweni	enclave
TU-36	amphibolite	Kotongweni	enclave
TU-37	amphibolite	Kotongweni	enclave
TU-38	amphibolite	Kotongweni	enclave
TU-39	hornblendite	Kotongweni	enclave
TU-40	gabbroic gneiss	Kotongweni	
TU-41a	tonalitic gneiss	Kotongweni	
TU-41b	amphibolite	Kotongweni	enclave
TU-42a	amphibolite	Kotongweni	enclave
TU-42b	amphibolite	Kotongweni	enclave
TU-43a	gabbroic gneiss	Kotongweni	
TU-43b	hornblendite	Kotongweni	enclave
TU-44a	amphibolite	Kotongweni	enclave
TU-44b	tonalitic gneiss	Kotongweni	
TU-45	talc schist	Kotongweni	extremely sheared
TU-46	talc schist	Kotongweni	extremely sheared
TU-47	talc schist	Kotongweni	extremely sheared
TU-48	talc schist	Kotongweni	extremely sheared
TU-49a	gabbro	Ntabasongoma	
TU-49b	gabbro	Ntabasongoma	
TU-50	gabbro	Ntabasongoma	
TU-51	gabbro	Ntabasongoma	
TU-52	felsic gneiss	Nkomo	
TU-53	felsic gneiss	Mandleni	
TU-54	amphibolite	Mandleni	
TU-55	marble	Mandleni	banded limestone
TU-56	amphibolite	Nkomo	
TU-57	pseudotachylite	Mambulu	Mambulu complex
TU-58	pseudotachylite	Mambulu	Mambulu complex

Appendix 2. Whole rock composition of gabbroic to tonalitic gneisses of the Kotongweni complex.

Sample No.	TU16b	TU43a	TU16a	TU31	TU32	TU40	TU44b	KR-MA	TU9
SiO2	44.71	47.52	47.78	52.56	52.96	54.37	58.58	59.16	60.79
TiO2	0.77	1.04	0.62	0.61	0.57	0.56	0.67	0.55	0.58
Al2O3	16.15	15.72	18.32	17.71	17.2	17.31	16.69	17.84	15.49
Fe2O3	16.13	14.05	14.07	12.47	11.99	11.76	10.29	7.67	8.66
MnO	0.25	0.24	0.22	0.2	0.2	0.19	0.14	0.1	0.17
MgO	6.64	5.96	4.96	4.28	3.9	3.3	2.45	2.14	2.35
CaO	11.38	11.39	10.98	10.14	9.46	11.04	7.96	7.91	7.25
Na2O	1.32	2.11	1.84	1.95	2.02	0.86	2.67	3.41	2.58
K2O	0.3	0.33	0.14	0.1	0.14	0.06	0.13	0.35	0.31
P2O5	0	0.56	0.08	0.11	0.09	0.22	0.21	0.11	0.1
Total	97.65	98.92	99.01	100.11	98.52	99.67	99.79	99.24	98.28
A.S.I.	0.70	0.64	0.79	0.81	0.83	0.80	0.88	0.88	0.87
XRF									
Ba	69.9	155.7	47.1	44.8	65.1	38.4	162.5	170.7	98.3
Co	41.5	34.5	39	31.1	32.2	27	27.9	19.5	23.6
Cr	25.4	21.5	16.3	29.8	27.6	25	18.2	19.2	16.2
Cu	123.4	37.2	119	82	108.1	59.5	21.3	15.9	26.6
Nb	1.4	1.1	1.8	0.8	0.8	0	0.6	1.6	2.9
Ni	13.5	1.2	12.1	9.5	8.3	7.6	8.8	3.5	5.1
Rb	5.4	6	4.8	2.8	1.6	2.7	5.4	10.7	5.7
Sr	211.2	278.9	289	283.7	280.2	319.8	340.3	345.3	270.7
V	448.1	177.5	329.9	265.6	249.8	228.9	258.2	125.7	156.9
Y	16.6	30.2	9.3	10.2	9.9	5.8	9.2	8.6	17.7
Zn	111.7	111.1	101.2	97.4	102.2	97	77.7	79	94.1
Zr	24.4	20.5	19.1	23.5	23.1	14.9	23.6	25.3	27.2
ICPM									
Li	5.91		5.48	4.63		2.74		5.60	
Be	0.24		0.26	0.29		0.22		0.58	
Rb	2.93		1.49	0.83		0.79		5.11	
Y	15.73		9.71	9.15		4.96		8.61	
Zr	17.39		8.82	11.79		3.17		12.80	
Nb	1.25		0.77	0.85		0.16		1.30	
Mo			0.16					0.11	
Sn			0.30					0.34	
Sb			0.03					0.11	
Cs			0.03					0.10	
La	1.49		4.84	1.68		1.59		1.90	
Ce	5.69		4.28	4.84		4.26		4.98	
Pr	1.04		0.71	0.77		0.63		0.75	
Nd	5.99		4.07	4.15		3.41		4.00	
Sm	2.00		1.40	1.27		0.96		1.35	
Eu	0.69		0.53	0.49		0.47		0.67	
Gd	2.31		1.55	1.46		1.04		1.53	
Tb	0.43		0.29	0.27		0.18		0.29	
Dy	2.85		1.91	1.76		1.05		1.73	
Ho	0.61		0.40	0.36		0.21		0.34	
Er	1.73		1.07	1.00		0.55		0.92	
Tm	0.28		0.16	0.15		0.08		0.14	
Yb	1.84		1.31	1.04		0.50		0.88	
Lu	0.30		0.16	0.16		0.08		0.13	
Hf	0.71		0.39	0.47		0.11		0.58	
Ta	0.05		0.03	0.04		0.01		0.07	
Tl			0.00					0.00	
Pb	3.51		1.73	1.69		2.26		6.44	
Th	0.02		0.03	0.05		0.06		0.09	
U	0.04		0.02	0.03		0.02		0.20	

Appendix 2. Whole rock composition of gabbroic to tonalitic gneisses of the Kotongweni complex (continued).

Sample No.	KR-33a	KR-43b	STJ96T4	TU10b	KR-46a	TU7a	TU15	KR-44a	TU34b
SiO2	61.2	61.74	62.22	64.74	66.37	66.86	67.15	68.49	68.69
TiO2	0.65	0.6	0.52	0.32	0.4	0.5	0.3	0.48	0.32
Al2O3	16.49	14.84	16.26	15.21	15.37	14.45	15.03	15.51	14.05
Fe2O3	8.15	9.53	8.24	6.8	5.57	6.97	5.28	4.58	6.63
MnO	0.1	0.37	0.23	0.13	0.09	0.12	0.07	0.09	0.12
MgO	2.25	2.14	1.99	2.49	1.38	1.96	1.31	1.22	2.02
CaO	7.49	6.55	6.93	6.66	6.16	6.23	6.2	5.85	6.4
Na2O	3.09	2.36	2.98	2.71	3.24	2.45	2.92	3.15	2
K2O	0.3	0.25	0.25	0.12	0.22	0.33	0.09	0.15	0.05
P2O5	0.1	0.11	0.08	0.06	0.05	0.06	0.06	0.05	0.11
Total	99.81	98.49	99.69	99.24	98.85	99.93	98.41	99.57	100.41
	0.87	0.92	0.91	0.91	0.92	0.92	0.93	0.97	0.94
XRF									
Ba	100.6	104.9	100.3	56.8	132.7	139.7	35.5	117	46.3
Co	20.7	22.6	19.6	17.8	15.3	16.8	13	11.1	17.9
Cr	10.3	18.7	16.2	33.8	17.5	9.9	1.1	4.5	24.3
Cu	32.2	12.1	40.7	12.1	25.4	14.4	9.4	16.5	14.1
Nb	3.1	1.1	1.7	2.2	1.3	2	1.5	1.1	0.4
Ni	3.8	0.6	4.3	9.8	4.5	2.6	0.7	3	3.3
Rb	4.4	4.1	3.7	3.2	5.3	10.2	2.8	2.6	0.6
Sr	281.7	222.3	266.5	289.7	287.7	251.7	298.7	298.4	290.8
V	129.8	129.9	118.6	145	106.4	124.9	79.2	94.1	108.7
Y	9.4	16.9	12.9	11.6	8.3	13.6	7.5	4.1	7.2
Zn	86.9	74.9	72.5	66.5	56.4	72.9	57.5	46.5	65.5
Zr	31.7	34.2	24.9	31.5	28.2	33.3	12.6	27.5	15.9
ICPM									
Li		3.59	4.68	4.09	2.70			4.86	
Be		0.74	0.41	0.36	0.48			0.46	
Rb		3.60	2.53	1.29	3.14			1.56	
Y		13.74	11.74	8.84	5.36			3.56	
Zr		18.44	16.13	24.20	12.72			17.60	
Nb		1.36	1.01	0.96	0.76			0.88	
Mo			0.22	0.10				0.13	
Sn			0.25	0.27				0.23	
Sb			0.13	0.19				0.09	
Cs		0.07	0.04	0.03	0.06			0.03	
La		1.30	1.73	2.04	1.10			1.38	
Ce		3.57	4.41	5.94	2.88			2.98	
Pr		0.57	0.69	0.93	0.43			0.42	
Nd		3.04	3.66	4.74	2.24			2.19	
Sm		0.99	1.22	1.39	0.72			0.72	
Eu		0.51	0.58	0.45	0.34			0.41	
Gd		1.49	1.52	1.47	0.96			0.81	
Tb		0.31	0.31	0.28	0.16			0.15	
Dy		2.18	2.08	1.73	1.02			0.81	
Ho		0.50	0.46	0.35	0.21			0.15	
Er		1.62	1.30	0.94	0.59			0.37	
Tm		0.24	0.22	0.15	0.08			0.05	
Yb		1.79	1.44	0.96	0.57			0.30	
Lu		0.28	0.22	0.15	0.08			0.04	
Hf		0.58	0.57	0.72	0.37			0.50	
Ta		0.07	0.05	0.04	0.04			0.05	
Tl									
Pb		1.60	3.80	4.33	1.47			4.05	
Th		0.06	0.06	0.10				0.14	
U		0.04	0.04	0.05				0.07	

Appendix 2. Whole rock composition of gabbroic to tonalitic gneisses of the Kotongweni complex (continued).

Sample No.	TU12a	TU11	TU12b	TU8b
SiO2	68.75	69.29	71.76	72.76
TiO2	0.43	0.55	0.32	0.17
Al2O3	14.61	14.34	13.91	14.77
Fe2O3	6.18	5.94	4.53	2.23
MnO	0.15	0.14	0.11	0.04
MgO	1.73	1.1	1	0.95
CaO	5.44	5.54	5.19	6
Na2O	3.04	2.95	3.08	3.22
K2O	0.2	0.14	0.09	0.11
P2O5	0.04	0.09	0.09	0
Total	100.55	100.08	100.07	100.25
	0.97	0.95	0.95	0.90
XRF				
Ba	189.6	138.5	105.7	126
Co	11.8	18.2	7.9	5.9
Cr	24.3	5.9	7.5	8.1
Cu	15.6	84.7	15.9	11.1
Nb	1.8	3.3	1.8	0.2
Ni	3.5	1.4	0.7	3.5
Rb	7.4	2.6	1.5	2.6
Sr	287.6	324.6	297.4	277.4
V	99.2	38.2	37.1	44
Y	22.9	9.9	11.7	5.9
Zn	88.1	65.2	62.4	21.3
Zr	32.5	49.2	29.5	31.2
ICPM				
Li		2.37	3.33	
Be		0.50	0.50	
Rb		1.55	0.84	
Y		8.57	9.99	
Zr		32.90	15.50	
Nb		1.93	0.66	
Mo		0.15	0.11	
Sn		0.30	0.24	
Sb		0.23	0.22	
Cs		0.05	0.03	
La		2.25	3.10	
Ce		6.17	7.67	
Pr		0.96	1.13	
Nd		4.98	5.85	
Sm		1.46	1.58	
Eu		0.86	0.76	
Gd		1.53	1.67	
Tb		0.27	0.30	
Dy		1.64	1.88	
Ho		0.34	0.38	
Er		0.91	1.07	
Tm		0.14	0.16	
Yb		0.92	1.07	
Lu		0.14	0.16	
Hf		0.90	0.49	
Ta		0.08	0.02	
Tl				
Pb		3.95	5.28	
Th		0.08	0.06	
U		0.06	0.04	

Appendix 3. Whole rock composition of enclave in the Kotongweni complex.

Sample No.	TU14a	TU7c	KR-40c	TU38	TU37	TU41b	TU44a	KR-44b	KR-40b	TU8a
	mafic enclave									
SiO2	48.05	49.45	53.50	42.99	45.27	45.46	46.14	48.87	48.89	50.91
TiO2	0.63	0.91	0.80	0.82	0.76	1.02	0.73	0.86	0.64	0.58
Al2O3	17.77	16.50	15.02	18.01	16.76	16.59	16.71	17.15	15.42	12.94
Fe2O3	13.74	14.75	12.04	16.98	16.43	12.75	15.61	14.24	12.57	10.04
MnO	0.25	0.28	0.23	0.29	0.30	0.21	0.28	0.22	0.21	0.18
MgO	5.62	4.64	4.49	4.9	6.25	9.27	6.54	4.61	6.93	8.65
CaO	10.98	8.97	8.55	12.82	11.68	11.39	11.64	9.68	10.32	15.39
Na2O	1.89	2.53	2.42	0.33	1.19	2.23	1.36	2.68	2.34	0.6
K2O	0.24	0.34	0.39	0.16	0.16	0.23	0.15	0.38	0.43	0.1
P2O5	0.00	0.08	0.03	0.09	0.08	0.04	0.07	0.08	0.19	0.09
total	99.18	98.44	97.47	97.38	98.87	99.19	99.21	98.77	97.94	99.5
XRF										
Ba	71.5	93.4	100.6	29.2	112.3	45.7	74.2	106.8	82.7	22.1
Co	36.4	36.5	20.7	38.2	43.6	52.8	47.3	35.2	41.4	37.2
Cr	22.7	27.8	10.3	28.8	32.6	75.3	21.5	25.4	96	423.9
Cu	278.9	112.5	32.2	67.3	122.7	29.9	178.0	110.6	11.1	31.5
Nb	1.5	2.8	3.1	1.3	0.0	5.3	1.4	1.3	2.9	2.1
Ni	13.5	8.1	3.8	12.7	22.4	143.3	33.5	7.5	30.7	75.9
Rb	5.5	6.9	4.4	3.4	4.1	3.3	3.4	5	5.4	2.9
Sr	251.1	243.2	281.7	371.2	311.6	240.4	309.4	223.3	295.9	300.2
V	369.7	326.5	129.8	560.5	381.5	235.6	406.9	357.9	322.4	230.5
Y	21.9	25.3	9.4	10.3	7.5	12.6	15.0	12.3	12.6	13.7
Zn	119.2	136.7	86.9	137.8	137.5	104.7	120.1	147.5	106.4	73
Zr	25.7	34.8	31.7	17.2	16.3	66.7	15.9	17.2	40.2	40.9
ICPM										
Li	5.52	9.87	11.62		5.39	8.05				1.27
Be	0.29	0.45	1.27		0.22	0.41				0.39
Rb'	3.07	2.67	3.89		2.03	1.69				0.89
Y'	18.85	22.21			6.34	12.23				11.70
Zr'	16.61	26.92	35.37		3.60	54.96				28.59
Nb'	1.26	2.17			0.24	4.30				0.90
Mo	0.24	0.23								
Sn	0.25	0.48								
Sb		0.14								
Cs	0.12	0.06	0.03							
La	1.79	2.36	2.57		2.01	3.48				4.05
Ce	6.12	7.69	9.29		3.62	8.92				9.69
Pr	1.13	1.39	1.90		0.57	1.41				1.39
Nd	6.70	8.15	11.84		3.16	7.19				6.90
Sm	2.35	2.68	5.04		1.06	2.09				1.81
Eu	0.78	0.78	1.48		0.56	0.81				0.66
Gd	2.64	3.14	7.49		1.18	2.32				1.98
Tb	0.54	0.63	1.45		0.21	0.40				0.35
Dy	3.50	4.05	8.08		1.35	2.51				2.24
Ho	0.74	0.86	1.64		0.28	0.50				0.47
Er	2.14	2.48	5.16		0.76	1.32				1.33
Tm	0.33	0.39	0.71		0.13	0.19				0.20
Yb	2.32	2.65	4.85		0.93	1.26				1.34
Lu	0.36	0.41	0.69		0.13	0.19				0.20
Hf	0.71	1.20	1.42		0.14	1.48				0.88
Ta	0.04	0.08	0.12		0.02	0.28				0.06
Pb	3.14	2.26	1.80		1.06	1.37				3.26
Th	0.04	0.04	0.10		0.09	0.31				0.39
U	0.02	0.03	0.10		0.03	0.08				0.24

Appendix 3. Whole rock composition of enclave in the Kotongweni complex (continued).

Sample No.	KR-41	TU43b	TU39	TU33	TU34a	KR-42a
	Hornblendite					metasediment
SiO2	49.03	49.31	50.62	51.85	54.54	62.27
TiO2	0.68	0.26	0.19	0.65	0.51	0.59
Al2O3	11.28	5.89	6.89	7.64	6.36	15.43
Fe2O3	10.41	8.46	15.68	15.17	14.08	7.59
MnO	0.21	0.14	0.39	0.32	0.34	0.13
MgO	12.25	16.41	15.57	12.81	13	2.21
CaO	10.85	18.16	9.97	10.2	9.5	6.43
Na2O	1.83	0.53	0.73	0.92	0.75	2.93
K2O	1.10	0.17	0.13	0.15	0.12	0.37
P2O5	0.22	0	0	0	0	0.08
total	97.87	99.33	100.17	99.69	99.19	98.02
XRF						
Ba	662.2	45.2	21.2	6.6	10.6	151.4
Co	43.6	49.5	55.6	50.4	49.1	20.5
Cr	1173.6	958.8	873.7	2121.5	2946	16.9
Cu	44.8	18.5	8.2	12.2	6.4	22.4
Nb	3.2	0.7	0.5	2.5	1.9	2
Ni	284.4	200.2	87.3	112.4	149.4	5
Rb	28.5	1.2	2.8	1.3	1.9	12.7
Sr	292.5	41.7	24.8	24.6	19.8	270.9
V	171.5	232.4	167.4	235.9	205.9	145.3
Y	16	2.9	12	36.8	26.6	14.7
Zn	128.7	38.5	148.6	136.4	141	80.7
Zr	56	5.1	9.6	30.3	22.8	26.7
ICPM						
Li		2.98			3.41	
Be		0.11			0.21	
Rb'		1.13			0.45	
Y'		3.00			22.13	
Zr'		2.11			19.50	
Nb'		0.05			1.49	
Mo						
Sn						
Sb						
Cs						
La		0.33			1.31	
Ce		0.91			6.64	
Pr		0.17			1.45	
Nd		0.98			8.88	
Sm		0.38			3.09	
Eu		0.17			0.76	
Gd		0.49			3.36	
Tb		0.10			0.63	
Dy		0.62			4.17	
Ho		0.13			0.87	
Er		0.34			2.43	
Tm		0.05			0.39	
Yb		0.31			2.61	
Lu		0.05			0.41	
Hf		0.12			0.92	
Ta		0.01			0.06	
Pb		2.77			2.92	
Th		0.03			0.04	
U		0.04			0.13	

Appendix 4. Amphibolite and gabbroic rocks in the Tugela sheet.

Sample No.	KR-51b	KR-51c	KR-32	KR-51d	KR-50b	KR-50a	STJ97T52	KR-50c	TU26
Description	manyane amphibolite (country rock)								
SiO2	46.31	48.27	48.87	49.18	50.25	50.59	50.90	52.48	48.49
TiO2	1.11	1.22	0.31	0.86	1.37	1.40	0.80	0.64	0.91
Al2O3	16.16	7.94	12.88	16.49	12.43	12.35	13.77	14.22	14.18
Fe2O3	12.7	13.65	11.51	10.31	17.48	17.37	11.84	11.53	12.74
MnO	0.2	0.24	0.16	0.2	0.25	0.25	0.18	0.17	0.20
MgO	5.96	13.88	8.68	6.37	5.08	5.04	7.47	5.67	7.17
CaO	11	12.64	12.73	10.88	9.51	9.43	11.57	9.04	12.44
Na2O	3.26	1.00	3.23	3.07	1.92	1.93	2.06	3.15	1.88
K2O	0.55	0.58	0.35	0.38	0.66	0.80	0.47	0.57	0.26
P2O5	0.5	0.00	0.02	0.34	0.10	0.11	0.02	0.03	0.05
total	97.75	99.42	98.74	98.08	99.06	99.25	99.08	97.50	98.32
XRF									
Ba	929.5	119.6	105.3	469.8	78.5	88.4	116.3	227.9	27.1
Co	39	59.1	50.5	36.8	50.1	48.5	46.9	35.6	50.2
Cr	88	598.2	675.7	127.5	32.2	34	256.8	121.9	209.9
Cu	29.1	16.9	59.8	76.3	64.3	62.4	105.4	28.9	131.4
Nb	2.8	10.7	1.1	2.8	2.4	2.8	1.7	0.8	1.4
Ni	33	108.8	118.7	38.7	24.3	23.6	73.9	20.7	77.3
Rb	4.4	5.8	4.8	4.3	10.4	8.4	9.0	7	4.8
Sr	1343.2	179.4	153.7	1386.4	98.7	91.7	110.2	367.3	122.0
V	323.9	350.2	283.6	232.2	429	423.3	264.2	329	298.5
Y	21.4	33.8	4.6	14	38.3	38.2	21.9	10.2	25.3
Zn	109.9	129.2	65.5	97.9	131.8	128.5	80.1	83.3	89.0
Zr	63.3	75.7	14.1	67.4	69	71.1	46.7	37.2	47.1
ICPM									
Li						5.16		3.71	
Be						0.00		0.35	
Rb						5.65		5.89	
Y						32.57		9.22	
Zr						66.56		26.17	
Nb						2.24		1.08	
Cs						0.02		0.11	
La						3.44		3.43	
Ce						8.77		5.53	
Pr						1.58		0.74	
Nd						8.14		3.60	
Sm						3.13		1.27	
Eu						1.25		0.70	
Gd						4.89		1.80	
Tb						0.99		0.33	
Dy						6.08		1.82	
Ho						1.29		0.37	
Er						3.94		1.09	
Tm						0.59		0.16	
Yb						4.17		1.07	
Lu						0.59		0.16	
Hf						2.11		0.75	
Ta						0.14		0.05	
Pb						0.90		1.89	
Th						0.46		0.42	
U						0.19		0.12	

Appendix 4. Amphibolite and gabbroic rocks in the Tugela sheet (continued).

Sample No.	TU28	TU29	TU18	TU30	TU22	TU24	TU25	TU23	TU19
Description						metagabbro			
SiO2	49.67	49.74	49.86	50.46	53.30	46.15	47.46	48.44	49.05
TiO2	1.12	1.55	0.94	0.82	0.62	0.49	0.54	0.67	0.47
Al2O3	13.44	14.79	13.94	16.25	14.49	11.42	13.41	16.63	13.10
Fe2O3	15.10	11.53	13.24	10.79	11.98	11.43	12.32	8.26	11.06
MnO	0.22	0.20	0.20	0.22	0.22	0.19	0.22	0.14	0.18
MgO	6.01	5.69	6.17	5.88	5.95	13.74	9.65	7.08	10.18
CaO	10.94	11.09	11.57	10.10	8.73	12.03	12.34	13.89	11.41
Na2O	1.89	2.83	2.39	3.07	3.13	1.38	1.82	2.39	1.70
K2O	0.39	0.46	0.23	0.46	0.45	0.53	0.37	0.22	0.31
P2O5	0.08	0.17	0.05	0.39	0.04	0.02	0.01	0.06	0.00
total	98.85	98.06	98.59	98.44	98.91	97.38	98.14	97.78	97.47
XRF									
Ba	351.3	290.4	33.5	498.4	119.8	133.1	68.7	64.6	107.9
Co	47.0	41.4	47.9	32.8	33.8	57.5	43.0	34.1	46.6
Cr	78.1	103.2	72.2	117.4	226.3	334.3	608.5	625.6	609.3
Cu	118.8	48.1	11.5	36.2	15.1	4.3	4.7	5.4	36.5
Nb	2.1	4.7	1.4	4.0	1.9	1.6	1.7	1.5	1.4
Ni	39.0	41.0	55.3	37.1	34.5	300.1	170.0	124.5	152.8
Rb	9.7	5.5	4.4	9.3	8.2	10.0	6.1	3.7	8.1
Sr	134.0	308.1	125.2	637.4	221.4	75.2	141.9	186.0	148.1
V	369.4	415.1	315.9	275.3	263.6	165.3	234.5	214.6	286.4
Y	29.1	28.4	25.7	25.2	10.0	15.0	15.1	15.9	10.4
Zn	107.6	123.4	93.5	124.7	98.1	50.8	69.5	43.6	69.5
Zr	58.9	58.4	45.0	42.9	30.8	31.7	32.1	40.5	28.1
ICPM									
Li			3.25	9.15	5.42			2.19	
Be			0.26	1.14	0.38			0.21	
Rb			2.24	6.18	6.11			2.37	
Y			22.76	22.17	9.75			14.01	
Zr			37.92	19.81	23.28			32.23	
Nb			1.23	3.02	0.92			1.05	
Cs									
La			1.85	19.24	1.97			2.02	
Ce			5.21	40.52	5.17			5.22	
Pr			0.88	5.30	0.78			0.81	
Nd			4.72	23.82	3.82			4.24	
Sm			1.88	5.46	1.21			1.45	
Eu			0.79	1.88	0.64			0.61	
Gd			2.75	5.42	1.46			1.94	
Tb			0.57	0.77	0.27			0.39	
Dy			3.94	4.57	1.79			2.63	
Ho			0.89	0.86	0.38			0.56	
Er			2.55	2.27	1.06			1.52	
Tm			0.40	0.32	0.17			0.24	
Yb			2.70	2.03	1.16			1.58	
Lu			0.42	0.31	0.18			0.23	
Hf			1.27	0.63	0.72			1.00	
Ta			0.08	0.17	0.05			0.07	
Pb			3.56	5.73	3.01			2.16	
Th			0.26	0.92	0.20			0.22	
U			0.10	0.38	0.08			0.10	

Appendix 4. Amphibolite and gabbroic rocks in the Tugela sheet (continued).

Sample No.	TU20	TU27	TU21	TU17p	TU17o	TU17a	TU17u2	TU17u1
Description			tonalite dyke	pillow lava in the Tuma slice				
SiO2	48.94	49.24	69.70	44.75	46.48	49.34	54.10	55.55
TiO2	2.31	1.86	0.34	0.61	0.58	0.50	0.60	0.42
Al2O3	14.95	14.99	14.12	17.52	15.76	17.57	13.15	15.44
Fe2O3	16.92	15.12	4.94	11.47	9.69	9.53	10.19	8.33
MnO	0.30	0.26	0.06	0.28	0.15	0.14	0.18	0.14
MgO	2.77	3.97	0.84	6.70	5.46	4.11	6.77	5.35
CaO	9.00	8.89	4.99	13.75	18.60	15.54	11.16	7.09
Na2O	2.82	3.34	3.68	1.84	1.61	1.53	2.50	5.18
K2O	0.31	0.44	0.16	0.27	0.04	0.08	0.15	0.18
P2O5	0.74	0.23	0.05	0.00	0.00	0.01	0.01	0.00
total	99.06	98.32	98.88	97.19	98.36	98.35	98.82	97.69
XRF								
Ba	88.8	121.1	130.5	15.0	14.0	26.4	60.7	138.8
Co	28.5	36.1	10.9	43.4	43.6	36.2	34.3	37.0
Cr	17.8	22.7	8.8	317.0	721.0	535.3	898.0	285.9
Cu	26.7	50.4	20.2	15.6	10.8	30.6	6.8	2.9
Nb	4.9	7.1	1.3	2.1	1.7	1.0	0.4	1.1
Ni	2.2	12.8	0.7	64.3	220.9	123.5	137.9	93.3
Rb	4.9	7.8	2.6	3.7	1.0	0.7	1.8	1.2
Sr	273.8	223.7	332.2	156.3	157.4	139.9	296.4	228.5
V	61.3	253.6	23.9	312.3	300.3	310.3	199.0	159.1
Y	59.0	39.7	18.7	26.4	11.0	11.1	19.6	11.6
Zn	117.4	127.6	40.0	112.7	71.4	66.4	59.2	53.5
Zr	38.3	86.4	87.8	27.1	23.3	24.1	37.6	29.6
ICPM								
Li					3.53		1.82	
Be					0.35		0.32	
Rb					0.53		0.98	
Y					9.93		17.19	
Zr					16.34		25.47	
Nb					1.07		0.32	
Cs								
La					1.80		2.68	
Ce					4.18		6.33	
Pr					0.58		0.97	
Nd					2.79		5.03	
Sm					0.92		1.63	
Eu					0.40		0.59	
Gd					1.15		2.05	
Tb					0.24		0.42	
Dy					1.71		3.01	
Ho					0.39		0.65	
Er					1.15		1.87	
Tm					0.19		0.30	
Yb					1.25		2.02	
Lu					0.19		0.32	
Hf					0.57		0.86	
Ta					0.05		0.03	
Pb					23.69		4.35	
Th					0.30		0.30	
U					0.33		0.05	

Appendix 5. Whole rock composition of amphibolite in the Madidima sheet.

Sample No.	KR-10	STJ97T24	STJ97T29	STJ97T42	STJ97T25	STJ97T40	KR-28	STJ97T24KR
SiO2	47.49	47.81	47.97	48.16	49.21	49.94	51.73	51.82
TiO2	0.08	0.41	1.02	1.18	0.36	0.13	0.42	0.56
Al2O3	14.31	14.36	14.51	16.36	14.95	9.51	18.39	17.3
Fe2O3	10.08	11.30	12.65	12.50	10.22	8.94	9.11	13.8
MnO	0.19	0.18	0.19	0.17	0.16	0.16	0.16	0.2
MgO	11.41	8.38	8.11	5.33	8.36	15.46	4.06	2.21
CaO	11.12	12.76	11.35	11.48	12.29	12.22	9.11	7.21
Na2O	0.95	0.89	2.43	2.42	2.04	1.22	4.64	3.8
K2O	1.87	1.43	0.88	0.49	0.33	0.55	0.44	0.62
P2O5	0	0.00	0.03	0.04	0.00	0.00	0.06	0.16
Total	97.5	97.51	99.13	98.13	97.92	98.13	98.12	97.68
XRF								
Ba	567.8	298.4	236.1	64.5	85.2	73.6	136.6	257.1
Co	54.4	46.7	50.1	46.7	46.1	51.5	34.3	33.2
Cr	109.7	187.5	241.2	36.0	345.3	458.2	60.7	12.1
Cu	-0.7	2.6	38.1	83.2	26.3	1.9	114.2	141.1
Nb	0.1	0.2	2.9	4.2	1.0	2.5	1.8	1.2
Ni	48.3	67.0	108.8	39.5	103.8	104.3	28.6	2.6
Rb	118.4	74.1	18.8	8.0	10.1	15.5	4	19.8
Sr	168.2	167.3	289.2	153.6	199.2	78.2	410.5	244.1
V	177.5	288.1	274.1	287.6	235.7	180.9	200.2	114.1
Y	2.3	11.9	19.1	20.9	9.8	4.5	10.9	12.5
Zn	48	50.7	85.2	79.5	52.7	48.0	68.5	81.3
Zr	7.1	17.5	59.8	67.1	15.2	7.0	38.2	26.8
ICP-Mas								
Li	15.24						6.35	
Be	0.11						0.35	
Rb	101.25						3.27	
Y	1.15						9.36	
Zr	0.78						28.03	
Nb	0.02						1.18	
La	0.22						9.22	
Ce	0.43						18.01	
Pr	0.06						2.08	
Nd	0.30						8.59	
Sm	0.11						1.76	
Eu	0.15						0.63	
Gd	0.27						1.84	
Tb	0.03						0.28	
Dy	0.21						1.79	
Ho	0.05						0.37	
Er	0.14						1.05	
Tm	0.03						0.16	
Yb	0.16						1.10	
Lu	0.03						0.17	
Hf	0.03						0.80	
Ta	0.01						0.07	
Tl								
Pb	4.08						10.09	
Th	0.01						2.39	
U	0.01						0.86	

Appendix 5. Whole rock composition of amphibolite in the Madidima sheet (continued).

Sample No.	KR-21	KR-22	STJ97T26
SiO2	52.13	52.29	57.07
TiO2	0.82	0.44	1.04
Al2O3	13.77	13.94	16.30
Fe2O3	10.8	9.32	7.71
MnO	0.19	0.16	0.11
MgO	7.47	6.74	3.82
CaO	10.01	12.48	5.78
Na2O	2.55	2.38	4.14
K2O	0.61	0.49	1.99
P2O5	0.03	0.14	0.39
Total	98.38	98.38	98.34
XRF			
Ba	92.1	131.3	1012.0
Co	47.4	38.9	24.1
Cr	218.5	301.3	59.6
Cu	5	3.2	45.3
Nb	4.5	1.3	18.4
Ni	104.9	65.9	29.6
Rb	5.5	9.8	62.2
Sr	401.5	206	1241.1
V	243.6	182	137.7
Y	14.6	9	19.7
Zn	90.4	62.2	73.0
Zr	60.2	22.1	206.2
ICP-Mas			
Li		5.56	
Be		0.14	
Rb		6.47	
Y		7.81	
Zr		14.03	
Nb		0.36	
La		1.91	
Ce		4.18	
Pr		0.58	
Nd		2.86	
Sm		0.90	
Eu		0.41	
Gd		1.09	
Tb		0.21	
Dy		1.43	
Ho		0.31	
Er		0.88	
Tm		0.14	
Yb		0.94	
Lu		0.15	
Hf		0.46	
Ta		0.02	
Tl			
Pb		9.09	
Th		0.24	
U		0.12	

Appendix 6. Whole rock composition of amphibolite in the Mandleni sheet.

Sample No.	KR-1b	KR-24	KR-7	KR-5a	KR-30a	STJ97T18	STJ97T19	KR-13c	KR-17
SiO2	44.49	45.15	45.44	46.01	46.26	46.93	47.02	47.17	48.23
TiO2	1.76	2.4	2.14	3.04	1.11	1.66	2.28	1.69	1.76
Al2O3	9.31	14.02	13.59	12.59	9.63	14.12	14.50	12.27	13.51
Fe2O3	13.28	14.3	14.01	15.5	14.32	12.48	13.79	15.43	12.98
MnO	0.18	0.2	0.17	0.21	0.38	0.16	0.19	0.19	0.17
MgO	14.95	6.82	6.84	5.27	12.27	7.87	4.94	6.31	6.92
CaO	12.07	11.52	11.31	8.8	11.78	11.63	11.81	10.63	9.63
Na2O	1.49	2.4	2.69	2.84	1	2.67	2.70	2.39	3.14
K2O	0.33	1.17	0.91	2.23	1.14	1.20	0.59	0.84	0.93
P2O5	0.09	0.2	0.15	0.3	0.06	0.10	0.19	0.13	0.13
Total	97.95	98.18	97.25	96.78	97.95	98.82	98.00	97.04	97.38
XRF									
Ba	0	150.3	128.1	644	296.5	153.0	125.7	134.5	99.5
Co	66.2	52	54.3	48.8	53.7	52.5	50.1	48.2	44.7
Cr	1067.9	74.1	455.9	84.1	1403.4	241.2	178.0	118.5	207.7
Cu	15	40.6	110.6	48.8	20.8	22.4	95.9	19.7	100.4
Nb	12.3	26	13.7	33	19.8	13.3	24.0	14.1	11.3
Ni	730.3	76.5	158.2	57.7	492.2	134.8	75.5	60.4	58.1
Rb	2.1	20.1	15.1	68.6	16.8	17.9	13.2	9.3	33.9
Sr	236.8	387.1	324.7	456	146.3	424.2	425.3	181.9	492
V	216.1	339.1	331.8	364.3	272.4	262.7	300.2	292.4	283.7
Y	15.4	18.6	22.7	34.4	14.9	18.4	24.8	23.6	19.7
Zn	94.4	97	115.8	104.9	202.4	88.3	105.8	112.4	96.4
Zr	97.9	122.4	135.5	215.4	78.2	103.0	155.9	125.1	115.7
ICP-Mas									
Li				10.11		8.30	12.10		
Be				1.48		0.78	0.90		
Rb				62.48		13.79	10.63		
Y				28.60		15.86	22.35		
Zr				197.49		84.15	136.02		
Nb				26.95		10.82	18.65		
La				21.40		10.97	16.58		
Ce				48.82		21.70	38.18		
Pr				6.46		3.28	5.03		
Nd				28.40		14.40	22.38		
Sm				6.54		3.53	5.26		
Eu				2.22		1.25	1.80		
Gd				6.85		3.73	5.41		
Tb				1.07		0.61	0.86		
Dy				6.32		3.58	4.96		
Ho				1.15		0.65	0.90		
Er				2.98		1.66	2.35		
Tm				0.42		0.23	0.33		
Yb				2.67		1.48	2.14		
Lu				0.39		0.21	0.30		
Hf				5.09		2.40	4.04		
Ta				1.67		0.68	1.21		
Tl									
Pb				3.02		6.24	3.43		
Th				2.04		0.67	1.51		
U				0.76		0.35	1.27		

Appendix 6. Whole rock composition of amphibolite in the Mandleni sheet (continued).

Sample No.	KR-14b	KR-13d	KR-1a	KR-13b	KR-15	STJ97T14	KR-30b	STJ97T45
SiO2	48.25	48.32	48.46	48.6	49.01	56.02	60.1	60.11
TiO2	2.23	1.93	2.16	2.26	1.86	0.60	0.51	0.42
Al2O3	12.37	12.53	12.49	12.49	13.5	17.65	16.15	15.35
Fe2O3	15.93	14.59	14.15	14.98	13.98	8.77	7.12	8.53
MnO	0.2	0.19	0.17	0.17	0.18	0.13	0.11	0.13
MgO	5.58	5.73	6.26	5.5	5.56	3.71	1.85	2.53
CaO	10.47	11.43	11.18	10.13	10.98	8.49	8.71	6.66
Na2O	2.25	2.16	2.36	2.57	2.38	3.42	2.78	4.21
K2O	0.52	0.69	1.19	0.57	1	0.21	0.49	0.78
P2O5	0.18	0.15	0.21	0.19	0.15	0.03	0.14	0.03
Total	97.98	97.71	98.63	97.46	98.59	99.03	97.96	98.75
XRF								
Ba	87.8	72.4	151.8	211.3	351.7	181.1	319.8	716.6
Co	47.1	44.3	47.6	45.9	42.2	28.7	21.2	26.4
Cr	114.9	79.1	273	76.5	77	39.4	21.4	28.4
Cu	27.2	40.8	32.4	41.2	49.6	79.6	67.5	45.7
Nb	16.1	13.1	16.4	16.3	14.8	2.3	3.8	3.3
Ni	44	54.2	130.5	50.6	50.5	17.8	2.4	8.4
Rb	10	7.6	39.5	12.3	21.8	3.4	3.6	5.7
Sr	236.7	261.1	588.7	256.5	332.2	247.6	656.1	396.5
V	349.6	319.1	293	342.2	284.4	171.4	122.6	190.9
Y	28.7	24.8	25.7	30.5	26.6	15.6	19	8.4
Zn	126.4	110.2	110.5	121.5	108.2	54.0	73.9	68.3
Zr	151.5	128.2	163.7	150.9	139.5	47.2	79.2	37.6
ICP-Mas								
Li								
Be								
Rb								
Y								
Zr								
Nb								
La								
Cc								
Pr								
Nd								
Sm								
Eu								
Gd								
Th								
Dy								
Ho								
Er								
Tm								
Yb								
Lu								
Hf								
Ta								
Tl								
Pb								
Th								
U								

Appendix 7. Whole rock composition of granitic gneiss.

sample No.	STJ97T27	STJ97T16	KR-13e	STJ97T37	KR-12b	KR-8a	STJ97T33	KR-16	STJ97T41	KR-31c
Description	grey gneiss	grey gneiss	granitic gnei:	felsite dyke	granitic gnei:	felsic gneiss	bi qtz diorite	felsic gneiss	bi leucogneis	felsic gneiss
SiO2	66.82	68.24	71.17	71.36	71.42	71.56	71.63	71.73	71.97	72.34
TiO2	0.55	0.39	0.07	0.34	0.08	0.08	0.27	0.14	0.27	0.1
Al2O3	16.08	14.78	15.64	11.96	14.19	15.15	15.32	15.85	15.58	13.38
Fe2O3	3.17	4.71	0.59	4.39	0.73	0.48	2.74	0.87	2.07	3.25
MnO	0.06	0.07	0.01	0.20	0.01	0.01	0.03	0.01	0.04	0.05
MgO	0.76	1.26	0.16	1.15	0.17	0.19	0.80	0.33	0.67	1.25
CaO	2.47	5.90	1.51	7.60	0.95	2.1	3.94	1.56	2.17	5.03
Na2O	2.39	3.24	5.59	1.72	3.37	5.81	4.36	5.82	4.73	3.67
K2O	6.46	0.28	3.21	0.81	6.56	1.75	0.58	2.41	3.33	0.37
P2O5	0.05	0.02	0	0.03	0	0	0.01	0	0.03	0.02
total	98.81	98.88	97.94	99.55	97.47	97.13	99.67	98.73	100.86	99.46
ASI	1.04	0.90	1.01	0.68	0.99	0.99	1.02	1.06	1.02	0.86
XRF*										
Ba	1288.3	80.0	2501.8	313.7	1430	591.3	642.8	1054.2	1529.7	425.9
Co	4.4	14.3	0.8	11.1	0.3	0.9	9.7	5.4	4.8	10.7
Cr	2.9	17.7	19.5	4.4	6.5	9.8	20.0	10.4	14.7	46.9
Cu	15.1	38.1	4	0.1	0.5	0	24.4	4.3	0.0	68.8
Nb	4.6	4.0	2.6	8.8	4.1	3.3	2.3	4.6	10.6	1.8
Ni	5.2	7.5	7	4.4	1.7	1.8	6.6	0.5	7.7	10.6
Rb	113.7	7.1	54.3	25.1	137.9	31.5	36.6	53	68.7	7.7
Sr	172.1	238.6	1081	320.5	507	1100.1	862.0	615.7	1224.4	434.7
V	3.1	76.4	3.8	35.8	1.5	4.8	36.1	2.6	16.0	51.5
Y	36.3	13.9	0.7	40.2	0.7	1.8	1.4	2.3	6.2	4.7
Zn	89.6	28.5	7.1	48.9	15.4	24.9	22.6	27.1	44.3	23.7
Zr	131.1	77.0	66.9	100.4	42	112.9	127.5	102.5	164.1	50.3
ICP-MS										
Li					1.46					3.30
Be					1.00					0.46
Rb					131.18					2.39
Y					0.58					4.85
Zr					24.54					36.25
Nb					2.78					1.34
La					1.00					3.93
Ce					1.96					6.53
Pr					0.23					0.83
Nd					1.02					3.32
Sm					0.28					0.73
Eu					0.48					0.39
Gd					0.25					0.83
Tb					0.03					0.14
Dy					0.14					0.89
Ho					0.02					0.19
Er					0.06					0.54
Tm					0.01					0.09
Yb					0.06					0.58
Lu					0.01					0.09
Hf					1.13					0.93
Ta					0.11					0.06
Pb					45.65					17.59
Th					0.74					1.10
U					1.04					0.30

* ASI: Al2O3/(Na2O+K2O+CaO)

Appendix 7. Whole rock composition of granitic gneiss (continued).

sample No.	KR-8b	STJ97T43	STJ97T44	STJ97T28	KR-1c	STJ97T13	KR-13a	STJ97T36	STJ97T20	KR-18e
Description	felsic gneiss	bi leucogneis	bi leucogneis	granitic gnei	felsic gneiss	mica feldspa	granitic gnei	calc-silicate	felds gneiss	ga-granite
SiO2	72.35	72.62	72.68	72.72	72.87	72.89	73.05	73.06	73.07	73.66
TiO2	0.08	0.13	0.13	0.10	0.08	0.07	0.07	0.14	0.12	0.11
Al2O3	15.31	15.51	15.69	14.76	15.44	15.28	15.47	15.04	15.76	14.92
Fe2O3	0.56	1.01	0.94	1.12	0.6	0.77	0.56	1.27	1.17	1.19
MnO	0.01	0.01	0.01	0.03	0.01	0.01	0.01	0.02	0.02	0.03
MgO	0.19	0.28	0.28	0.29	0.21	0.20	0.19	0.33	0.30	0.27
CaO	2.1	1.34	1.47	1.77	1.56	1.37	1.39	1.42	2.09	1.58
Na2O	6.18	5.81	5.72	4.37	5.41	5.23	5.21	5.81	5.90	3.63
K2O	1.22	2.93	2.72	3.66	2.85	3.43	3.5	2.06	1.71	4.64
P2O5	0	0.00	0.00	0.00	0	0.00	0	0.00	0.00	0.01
total	97.98	99.64	99.63	98.80	99.02	99.25	99.46	99.14	100.14	100.04
ASI*	1.00	1.02	1.04	1.03	1.04	1.03	1.04	1.05	1.03	1.08
XRF										
Ba	396.4	1448.8	2257.5	3000.5	1011.3	2833.9	3059.1	813.9	518.4	798.7
Co	0	2.9	1.3	2.6	0	0.2	0.7	2.5	3.7	1.9
Cr	10.6	9.0	9.7	11.3	12.5	14.3	3.8	10.5	11.6	8
Cu	1.9	3.1	0.0	30.1	10.7	6.7	4.1	0.0	2.9	3.9
Nb	3	2.3	2.4	18.1	3.6	4.1	3.8	4.2	5.5	20.3
Ni	1.3	5.3	3.1	5.8	2.5	3.1	1	2.5	4.6	1.8
Rb	26.8	57.1	45.4	56.5	50.1	59.7	60.9	48.0	38.1	108.2
Sr	1013.9	1117.7	1296.1	1099.0	828.3	956.4	1014.3	468.6	1000.5	348.6
V	5.5	12.3	2.7	11.4	2.1	8.1	4.3	2.5	11.9	6.9
Y	2.4	1.0	1.6	9.4	1.1	0.8	0.6	4.4	3.6	10
Zn	24.2	29.8	44.1	28.8	11.5	13.4	9.5	29.8	40.2	48.6
Zr	104.2	118.4	135.3	72.5	67.9	90.0	88.1	88.7	108.5	73.6
ICP-MS										
Li					3.64		4.98			4.10
Be					2.10		1.35			2.32
Rb					43.00		53.64			94.66
Y					1.07		1.33			8.26
Zr					42.67		51.83			46.31
Nb					2.78		2.84			17.21
La					2.24		3.90			20.13
Ce					3.38		6.75			33.76
Pr					0.43		0.78			3.59
Nd					1.59		2.95			12.64
Sm					0.34		0.60			2.44
Eu					0.42		0.73			0.67
Gd					0.34		0.57			2.34
Tb					0.04		0.06			0.29
Dy					0.25		0.29			1.73
Ho					0.04		0.05			0.28
Er					0.11		0.12			0.71
Tm					0.01		0.02			0.10
Yb					0.12		0.11			0.66
Lu					0.01		0.01			0.08
Hf					1.76		1.55			1.53
Ta					0.10		0.16			1.34
Pb					24.52		21.53			21.89
Th					1.03		1.67			8.55
U					1.55		1.09			2.42

* ASI: Al2O3/(Na2O+K2O+CaO)

Appendix 7. Whole rock composition of granitic gneiss (continued).

sample No.	STJ97T10	STJ97T31	STJ97T38	STJ97T32	STJ97T17	STJ97T30
Description	granitic gnei	granitic gnei	grey gneiss	felds gneiss	granitic gnei	felds gneiss
SiO2	73.95	74.61	74.99	75.25	76.40	77.96
TiO2	0.03	0.03	0.30	0.29	0.06	0.24
Al2O3	15.43	14.56	13.23	13.21	14.34	12.15
Fe2O3	0.51	0.81	3.01	2.93	0.68	2.11
MnO	0.01	0.01	0.07	0.08	0.01	0.06
MgO	0.13	0.14	0.78	0.74	0.28	0.57
CaO	0.98	0.96	2.60	2.51	0.61	2.33
Na2O	5.41	5.08	4.45	4.34	6.83	3.93
K2O	3.86	3.57	0.98	1.18	0.46	1.14
P2O5	0.00	0.00	0.03	0.01	0.00	0.00
total	100.31	99.78	100.44	100.54	99.67	100.48
ASI*	1.04	1.04	1.01	1.02	1.12	1.02
XRF						
Ba	482.7	723.7	772.1	869.6	290.2	598.6
Co	0.9	1.1	6.9	8.3	2.7	4.4
Cr	6.7	13.2	10.1	10.1	23.8	17.3
Cu	2.6	3.1	1.1	0.8	21.6	4.8
Nb	3.1	2.4	3.8	3.8	9.5	4.3
Ni	4.1	3.4	4.1	2.8	12.7	6.4
Rb	89.5	55.8	31.4	26.9	21.1	24.1
Sr	460.6	325.0	248.4	216.4	370.2	131.2
V	4.7	4.7	25.0	23.6	7.3	9.3
Y	1.3	8.8	25.9	28.7	10.9	30.3
Zn	10.7	20.2	31.2	43.4	12.0	101.0
Zr	27.3	58.7	107.9	103.8	83.6	163.8
ICP-MS						
Li						
Be						
Rb						
Y						
Zr						
Nb						
La						
Ce						
Pr						
Nd						
Sm						
Eu						
Gd						
Tb						
Dy						
Ho						
Er						
Tm						
Yb						
Lu						
Hf						
Ta						
Pb						
Th						
U						

* ASI: Al2O3/(Na2O+K2O+CaO)

Appendix 8. Whole rock composition of ultramafic rocks in the Mandleni sheet.

Sample No.	STJ97T21	STJ97T34	STJ97T35	STJ97T23	STJ97T22	STJ97T46
SiO2	35.28	38.06	39.89	43.61	52.16	59.01
TiO2	0.01	0.56	0.01	0.02	0.05	0.01
Al2O3	0.10	24.11	0.18	1.23	4.60	0.51
Fe2O3	8.38	11.00	9.70	7.49	8.01	7.30
MnO	0.11	0.15	0.09	0.10	0.16	0.10
MgO	37.84	0.37	41.72	22.09	19.01	30.77
CaO	1.49	22.00	1.32	15.25	13.29	0.25
Na2O	0.00	0.09	0.00	0.00	0.48	0.00
K2O	0.00	0.13	0.00	0.00	0.13	0.01
P2O5	0.00	0.05	0.00	0.00	0.00	0.00
Total	83.21	96.52	92.89	89.80	97.89	97.95
XRF						
Ba	1.3	30.6	80.5	19.1	29.7	25.1
Co	96.2	14.1	88.0	72.6	54.3	79.5
Cr	3572.9	0.0	6079.3	2330.4	1661.1	3485.7
Cu	0.0	9.7	0.0	36.8	1.6	5.5
Nb	0.8	4.8	1.1	0.0	0.1	0.0
Ni	1541.6	5.1	2122.6	499.8	193.8	1040.0
Rb	1.4	8.9	4.3	0.6	1.9	1.1
Sr	17.8	592.2	19.4	52.0	11.2	5.6
V	19.7	99.4	22.8	47.3	151.4	13.4
Y	1.1	60.0	0.0	0.7	1.2	0.3
Zn	43.6	6.5	48.5	32.8	31.4	77.1
Zr	3.2	474.3	2.4	7.1	3.4	1.7

Appendix 9. Whole rock composition of several late stage intrusions in the Tugela terrane.

	Ntabasongoma gabbro			Mkondene diorite gneiss				
sample No.	TU51	TU50	TU49b	TU49a	STJ96T1	STJ96T8	STJ96T2	STJ97T51
Description	gabbro	gabbro	gabbro	gabbro	hyp bi diorite	hbl qtz diorite	bi qtz diorite	bi opx diorite
SiO2	45.79	47.07	47.21	49.14	55.31	59.47	61.32	61.69
TiO2	0.68	0.25	1.28	0.97	0.76	0.74	0.73	0.71
Al2O3	11.02	21.07	18.55	17.79	16.68	16.75	16.83	16.34
Fe2O3	10.18	5.08	11.02	10.50	8.07	6.75	6.37	6.50
MnO	0.13	0.07	0.14	0.14	0.11	0.12	0.09	0.10
MgO	13.78	7.21	4.95	5.05	4.47	2.91	2.23	2.19
CaO	15.80	15.27	8.92	8.80	7.70	5.91	5.11	4.77
Na2O	0.46	1.24	3.66	3.89	3.53	3.74	2.99	3.14
K2O	0.22	0.36	1.30	0.91	1.82	2.18	2.60	2.40
P2O5	0.04	0.04	0.55	0.46	0.40	0.27	0.24	0.24
total	98.08	97.66	97.57	97.63	98.83	98.83	98.51	98.08
XRF								
Ba	158.4	337.3	1079.2	1374.1	831.5	1648.0	1563.5	2009.7
Co	49.0	27.6	32.9	34.0	29.8	20.7	19.1	19.0
Cr	550.1	202.2	7.9	38.3	62.3	29.1	18.1	36.4
Cu	60.9	8.5	299.0	229.1	90.4	15.7	0.1	4.6
Nb	1.1	1.6	9.0	4.6	10.4	9.7	10.9	11.4
Ni	147.5	93.9	24.2	35.3	45.3	17.0	13.3	13.1
Rb	5.5	11.3	41.7	24.1	60.2	53.3	95.0	75.8
Sr	692.6	1330.4	1585.0	1327.3	1064.2	674.3	592.3	572.2
V	206.1	73.3	267.2	254.1	174.4	135.9	127.2	96.1
Y	9.0	3.3	20.4	16.1	16.1	16.1	15.2	16.1
Zn	54.6	35.7	112.1	99.5	84.3	77.8	73.0	74.1
Zr	49.9	73.3	131.5	100.5	231.3	209.8	230.5	271.3
ICPM								
Li	1.50			4.00	7.71		9.10	
Be	0.29			1.00	1.79		2.27	
Sc					17.09		18.31	
Rb	3.30			18.80	47.32		89.92	
Sr					1064.00		592.00	
Y	8.21			13.64	14.07		14.22	
Zr	25.28			59.70	183.67		232.46	
Nb	0.91			3.66	9.82		10.06	
Cs					0.97		2.58	
Ba					868.05		1339.25	
La	6.87			28.34	38.56		22.45	
Ce	18.45			59.01	85.80		46.54	
Pr	2.99			7.29	10.09		5.13	
Nd	15.42			30.64	38.61		19.61	
Sm	3.81			5.88	6.67		3.75	
Eu	1.16			1.88	1.61		1.14	
Gd	3.22			5.23	4.56		3.16	
Tb	0.41			0.59	0.58		0.42	
Dy	2.18			3.24	3.03		2.22	
Ho	0.34			0.55	0.53		0.42	
Er	0.82			1.39	1.44		1.12	
Tm	0.11			0.20	0.20		0.16	
Yb	0.66			1.26	1.31		1.16	
Lu	0.09			0.18	0.19		0.16	
Hf	1.06			1.65	4.17		4.72	
Ta	0.05			0.18	0.33		0.43	
Pb	6.95			8.16	15.02		17.48	
Th	0.80			3.60	3.13		1.29	
U	0.25			1.07	0.97		0.85	

Appendix 9. Whole rock composition of several late stage intrusions in the Tugela terrane (continued).

	Mambulu anorthosite complex			Tugela Rand	Mapumulo	Matigulu		
sample No.	STJ96T10A	STJ97T12	STJ97T11	STJ97T50	STJ96TT3	STJ96TT13B	STJ96TT8	STJ96TT12
Description	anorthosite	gabbronorite	anorthosite	pyroxenite	metabasite	tonalite gneiss	hbl-plag gneiss	granitic dyke
SiO2	50.77	52.47	53.24	42.68	50.92	66.42	70.79	75.32
TiO2	0.84	0.46	0.12	0.19	0.87	0.51	0.36	0.07
Al2O3	11.30	19.88	27.78	1.94	18.33	14.63	13.83	14.85
Fe2O3	8.70	5.00	1.08	10.63	10.72	7.55	4.28	1.03
MnO	0.16	0.09	0.01	0.14	0.18	0.14	0.07	0.01
MgO	10.20	4.54	0.22	33.76	4.19	2.00	1.72	0.31
CaO	13.65	12.20	10.69	5.27	8.82	4.60	5.74	3.14
Na2O	1.85	3.73	4.97	0.01	2.82	3.46	3.70	5.07
K2O	0.40	0.35	0.61	0.00	1.50	1.29	0.46	0.35
P2O5	0.00	0.00	0.00	0.00	0.12	0.03	0.05	0.00
total	97.87	98.73	98.72	94.62	98.47	100.62	101.00	100.16
XRF								
Ba	105.3	191.8	228.7	8.8	268.8	279.8	132.6	242.2
Co	42.7	24.4	1.9	100.1	33.6	20.5	12.0	5.2
Cr	236.6	30.3	5.2	3114.6	49.3	17.0	12.4	16.2
Cu	60.7	4.6	4.9	343.4	93.2	3.3	2.0	35.5
Nb	2.5	0.6	0.6	0.2	2.6	4.3	3.6	0.3
Ni	89.7	8.7	3.7	1684.6	19.8	4.7	5.0	6.7
Rb	6.2	3.2	10.0	3.1	65.7	37.2	11.7	9.0
Sr	220.4	815.6	1081.2	20.8	870.3	145.6	202.4	660.8
V	278.2	99.6	0.0	95.5	163.1	110.7	74.9	11.2
Y	16.9	7.3	1.2	3.5	24.9	40.1	18.4	1.1
Zn	41.8	24.5	4.2	63.7	110.8	63.6	23.1	6.3
Zr	34.6	34.6	35.4	6.4	85.6	70.4	55.0	125.8
ICPM								
Li								
Be								
Sc								
Rb								
Sr								
Y								
Zr								
Nb								
Cs								
Ba								
La								
Ce								
Pr								
Nd								
Sm								
Eu								
Gd								
Tb								
Dy								
Ho								
Er								
Tm								
Yb								
Lu								
Hf								
Ta								
Pb								
Th								
U								